



저작자표시-비영리-변경금지 2.0 대한민국

이용자는 아래의 조건을 따르는 경우에 한하여 자유롭게

- 이 저작물을 복제, 배포, 전송, 전시, 공연 및 방송할 수 있습니다.

다음과 같은 조건을 따라야 합니다:



저작자표시. 귀하는 원저작자를 표시하여야 합니다.



비영리. 귀하는 이 저작물을 영리 목적으로 이용할 수 없습니다.



변경금지. 귀하는 이 저작물을 개작, 변형 또는 가공할 수 없습니다.

- 귀하는, 이 저작물의 재이용이나 배포의 경우, 이 저작물에 적용된 이용허락조건을 명확하게 나타내어야 합니다.
- 저작권자로부터 별도의 허가를 받으면 이러한 조건들은 적용되지 않습니다.

저작권법에 따른 이용자의 권리는 위의 내용에 의하여 영향을 받지 않습니다.

이것은 [이용허락규약\(Legal Code\)](#)을 이해하기 쉽게 요약한 것입니다.

[Disclaimer](#)

THE THESIS FOR THE DEGREE OF MASTER SCIENCE

**Study on conversion of glucose and
xylose to furan derivatives using the
modified solid acid catalysts**

고형 산촉매 개질을 통한 글루코오스 및
자일로오스 유래 퓨란계 화합물
전환 연구

Advisor Professor: In-Gyu Choi

By Jong-Hwa Kim

PROGRAM IN ENVIRONMENTAL MATERIALS SCIENCE
DEPARTMENT OF FOREST SCIENCES
GRADUATE SCHOOL

AUGUST, 2017

Abstract

Study on conversion of glucose and Xylose to furan derivatives using the modified solid acid catalysts

Jong-Hwa Kim

Department of Forest Sciences

Graduate School

Seoul National University

Furan derivatives is considered as value added-chemical due to its high valorization to chemical or biofuel. Especially, Ethoxymethyl furfural (EMF) and Alkoxymethyl furan are considered as promising biofuel due to its high fuel properties (EMF: 8.7 kWh/l, alkoxymethyl furan: 27 MJ/kg) compared to bioethanol (6.1 kWh/l, 20 MJ/kg).

In this study, one-pot conversions from glucose to EMF and xylose to alkoxymethyl furan were conducted. Brønsted acid Amberlyst 15 and Lewis acid tin impregnated zeolite beta (Sn-BEA) were adopted in one-pot conversion reaction. Zeolite beta (NH₄-BEA) was modified to Sn-BEA by dealumination followed by tin impregnation. By zeolite modification, micropores surface area increased, while mesopores area, pore volume, and pore diameter remained. By XRF analysis, Si/Al ratio increased after dealumination process from 38 to 520. X-ray diffraction pattern was remained

constantly after zeolite modification process. Acidic properties of solid acid catalysts (zeolite, Amberlyst 15) were measured by Temperature-programmed desorption analysis. NH_3 molecules were used for probe molecule, indicating that Brønsted acidity of zeolite decreased by modification process.

One-pot conversion of glucose to EMF conducted at reaction temperature from 180 to 200 °C, reaction time from 10 to 30 min. Sn-BEA (0.025 g) with Amberlyst 15 (0.025 g), Amberlyst 15 (0.05 g), and Sn-BEA (0.05 g) used as catalysts. Maximum yield of EMF (29.37%) achieved by 190 °C of reaction temperature, 10 min of reaction time, and Sn-BEA with Amberlyst 15 as a catalyst. Lewis/Brønsted acidity ratio was changed in 190 °C of reaction temperature and 10 min of reaction time. As a result, Sn-BEA (0.025 g) with Amberlyst 15 (0.025 g) performed highest EMF yield. Alkoxyethyl furan conversion from furfural conducted at reaction temperature from 170 to 190 °C, 10 min of reaction time, and Sn-BEA (0.05 g) as a catalyst. Highest alkoxyethyl furan yield (36.73%) achieved at 190 °C of reaction temperature. One-pot conversion of xylose to alkoxyethyl furan conducted at reaction temperature from 170 to 190 °C, 10 min of reaction time, and Sn-BEA (0.025 g) with Amberlyst 15, Amberlyst 15 (0.05 g) and Sn-BEA (0.05 g) used as catalysts. The results showed that there was no alkoxyethyl furan production from xylose in one-pot conversion reaction in all reaction condition due to formation of propylene and lactate.

Reusability of Sn-BEA conducted by estimating activity of furfural to alkoxyethyl furan conversion. Catalytic activity remained until two time uses, and slightly decreased in three time uses.

Key words: glucose, xylose, one-pot reaction, EMF, alkoxyethyl furan, beta zeolite, Amberlyst 15, zeolite modification

Student number: 2015-23019

Contents

1. Introduction.....	1
1.1. Lignocellulosic biomass as alternative resources.....	1
1.2. Concept of biorefinery.....	2
1.3. Furan derivatives as a promising chemicals.....	4
1.4. Objectives.....	6
2. Literature reviews.....	7
2.1. EMF production from various feedstocks.....	7
2.1.1. 5-HMF to EMF conversion.....	7
2.1.2 Fructose to EMF conversion.....	9
2.1.3. Glucose to EMF conversion.....	9
2.2. Alkoxyethyl furan production from various feedstocks.....	12
2.2.1. Furfuryl alcohol to alkoxyethyl furan conversion.....	12
2.2.2. Furfural to alkoxyethyl furan conversion.....	12
2.2.3. Xylose to alkoxyethyl furan conversion.....	15
2.3. Acidic properties of zeolite.....	17
2.3.1. Lewis and Brønsted acidity on zeolite.....	17
2.3.2. Zeolite modification.....	18
3. Materials and methods.....	19
3.1. Materials.....	19
3.2. Catalysts preparation.....	19
3.2.1. Zeolite modification.....	19
3.3. Catalyst properties analysis.....	20
3.3.1. BET surface area and pore volume analysis.....	20
3.3.2. Powder X-ray diffractometry (XRD) analysis.....	20
3.3.3. Wavelength dispersive X-ray fluorescence (WDXRF) analysis.....	21
3.3.4. Temperature-programmed desorption (TPD) analysis.....	21

3.4. Reaction studies.....	22
3.4.1. One-pot conversion of glucose to EMF.....	22
3.4.2. Glucose to EMF conversion reaction by changing solid catalyst ratio.....	22
3.4.3. Furfural to alkoxyethyl furan conversion reaction.....	23
3.4.4. One-pot conversion of xylose to alkoxyethyl furan.....	23
3.4.5. Zeolite reusability test.....	23
3.5. Analysis of liquid fraction.....	24
3.5.1. Analysis of liquid fraction of glucose conversion reaction.....	24
3.5.2. Analysis of liquid fraction of furfural and xylose conversion reaction.....	25
4. Results and discussion.....	26
4.1. Physicochemical properties of zeolites.....	26
4.2. Acidic properties of solid acid catalysts.....	29
4.3. One-pot conversion of glucose to EMF.....	31
4.3.1. EMF yield versus reaction condition.....	31
4.3.1.1. Reaction temperature at 180 °C.....	31
4.3.1.2. Reaction temperature at 190 °C.....	35
4.3.1.3. Reaction temperature at 200 °C.....	38
4.3.2. EMF yield versus Lewis/Brønsted acid ratio.....	40
4.4. Conversion of furfural to alkoxyethyl furan.....	42
4.5. One-pot conversion of xylose to alkoxyethyl furan.....	44
4.6. Catalyst reusability.....	47
5. Conclusion.....	48
6. References.....	50

List of Tables

Table 1. Physicochemical properties of zeolites.....	27
--	----

List of figures

Figure 1. Scheme of integrated biorefinery concept.....	3
Figure 2. Proposed reaction mechanism from glucose to EMF.....	11
Figure 3. Proposed reaction pathway of furfural conversion by acid catalyst	16
Figure 4. Exhibition of Lewis acid sites on zeolite.....	17
Figure 5. X-ray diffraction patterns of NH ₄ -BEA and Sn-BEA.....	28
Figure 6. NH ₃ -TPD profile of zeolites and Amberlyst 15.....	30
Figure 7. EMF yield at reaction temperature 180 °C	34
Figure 8. EMF yield at reaction temperature 190 °C	37
Figure 9. EMF yield at reaction temperature 200 °C	39
Figure 10. Glucose to EMF products distribution by changing Lewis/Brønsted acid ratio.....	41
Figure 11. Contents of alkoxyethyl furan, and isopropyl levulinate after reaction of furfural conversion.....	43
Figure 12. Xylose to alkoxyethyl furan products distribution in 2-propanol.....	46
Figure 13. Alkoxyethyl formation by reuse Sn-BEA.....	47

1. Introduction

1.1. Lignocellulosic biomass as alternative resources

Energy consumption has been rapidly increased since the industrial revolution. Especially, fossil fuel occupies 80% of the total global energy, of which 58% alone is consumed by transport sector (Escobar et al., 2009). However, excessive use of fossil fuel leads to crisis of fossil fuel depletion (Agarwal, 2007) and undesired gas emission such as carbon dioxide. This gas gives rise to serious environmental problem, for example, climate change, rise in sea level, and air pollution (Singh et al., 2010). Also oil price has fluctuated depending on political issues (Ogbonna et al., 2001), there might be possibility to sharp rise of oil price in the future. Therefore, to overcome the drawbacks of fossil fuel utilization, investigation of an alternative fuel has urgently required (Zhang et al., 2016).

Among the alternative energy sources, lignocellulosic biomass has attracted interest because it is considered as renewable, abundant and carbon-neutral resource. Moreover, lignocellulosic biomass is being recognized as a promising resource due to its carbon rich property for conversion to transportation fuel or value-added chemicals that are conventionally produced in petroleum refinery (Kumar et al., 2009). According to United States Department of Energy, they set a goal for biomass to occupy 5% of total industrial and electrical generation energy demand, 20% of transportation fuel consumption, and 25% of biobased chemicals and materials in 2030 (Zhang et al., 2016). And European Union (EU) National Renewable Energy Action Plan set a goal to bioenergy to 12% of total energy consumption in 2020 (Johnston & van Kooten, 2015). Therefore, lignocellulosic biomass to biofuel becomes promising research field (Octave & Thomas, 2009).

1.2. Concept of biorefinery

The definition of biorefinery is an integrated facility that can produce fuels, power, and chemical from biomass. In the early bioenergy production, edible biomass were used as feedstock such as corn-grain or sugarcane, and they produced only bioethanol. Later not only ethanol but also fructose syrup, starch, corn oil, and corn glucan from the food sources were produced (Kamm & Kamm, 2004). However, utilization of the edible resources (eg. Corn-grain or sugarcane) had critical limitation in biorefinery due to the limitation of edible resources as feedstock problems such as food cost and morale issues. To overcome it, lignocellulosic biomass based biorefinery so-called 'integrated biorefinery' was developed and became promising process because lignocellulosic biomass are free from moral issues and cost problems. Also, lignocellulosic biomass comprise of various component such as cellulose, hemicellulose, and lignin and then each component can be applied to various industry as shown in Figure. 1 (Octave & Thomas, 2009). For example, cellulose and hemicellulose can be used as precursor for sugar derived products such as succinic acid and lactic acid, which are important precursors of chemical industry, also sorbitol and xylitol can be used for plasticizer (Octave & Thomas, 2009). And furan compounds derived from sugar are converted to versatile products (Alonso et al., 2010). Meanwhile, lignin can be used as adhesive, dispersing agents, flocculent, thickener, and precursor of BTX (benzene, toluene, xylene) (Octave & Thomas, 2009). Yet, the utilization of lignocellulic biomass based biorefinery is far feasibility due to its complex structure. Therefore, it is important to find the way not only to break complex structures of biomass effectively with improvement of economic value by using all component of biomass but to produce value added chemicals derived from sugars and lignin.

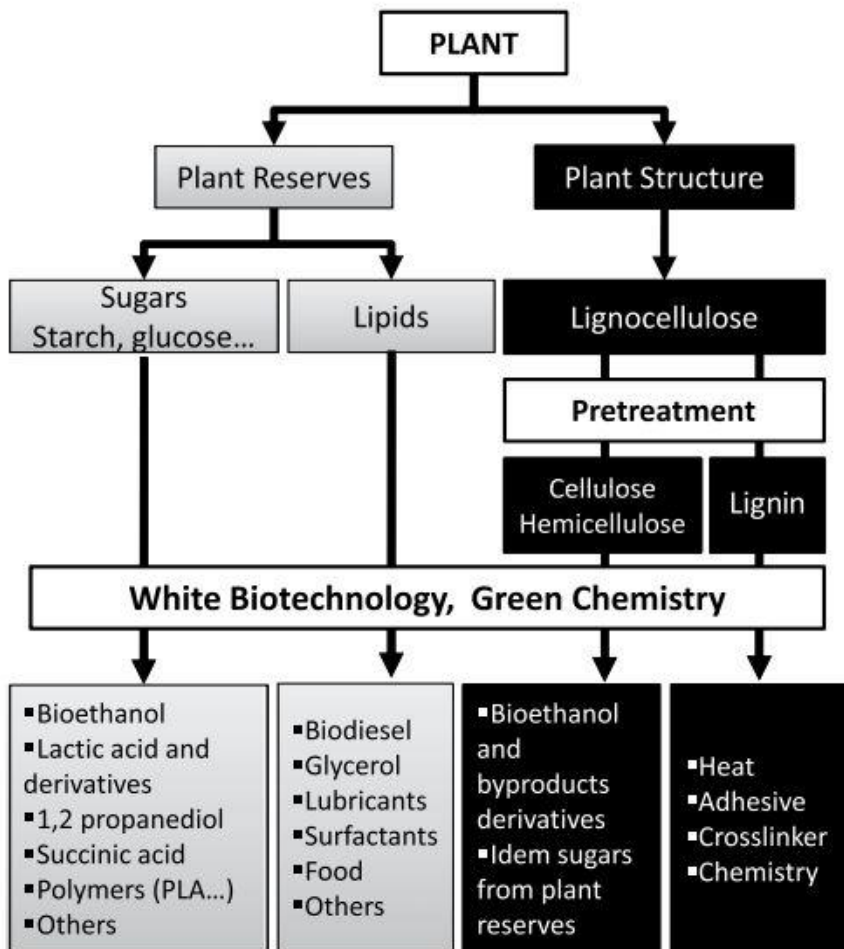


Figure 1. Scheme of integrated biorefinery concept (Octave & Thomas, 2009).

1.3. Furan derivatives as a promising chemicals

Both cellulose and hemicellulose, consisting mainly of glucose (C6) and xylose (C5) are degraded and converted to furan derivatives such as 5-hydroxymethylfurfural (5-HMF) and furfural during chemical pretreatment (Carrasquillo-Flores et al., 2013). And both furan derivatives are promising as potential chemicals that can replace organics from petroleum refinery (Yang & Sen, 2011). For example, furfuryl alcohol derived from furfural can be used for production of furan resin and solvents (Corma et al., 2007). Meanwhile 2,5-furandicarboxylic acid (FDCA) derived from 5-HMF can be used for polymer industry (Zhang & Deng, 2015). Moreover, furan derivatives can be typically used as potential additives for biofuel. Compared to bioethanol, biofuel derived from furan derivatives exhibits higher energy density, higher boiling point, and better lubricity (Roman-Leshkov et al., 2007).

Generally, furfural and 5-HMF are commonly used as starting materials for biofuel production. From furfural, 2-methyltetrahydrofuran (2-MTHF), which is applied to P-series fuel can be synthesized via hydrogenation reaction (Cho et al., 2014). And 2-Methylfuran (MF), which is a promising biofuel, also derived from hydrogenolysis reaction of furfural (Stevens et al., 2010). Also 4-(2-furyl)-3-buten-2-one (Fac) can be obtained by aldol reaction of furfural with acetone, and it can be adopted as a transportation fuel by hydrogenation. Furthermore, controlling carbon number is possible via further condensation reaction (Xu et al., 2011). Alkoxymethyl furan, which is converted from furfuryl alcohol by etherification with alcohol, is also attractive biofuel due to higher fuel properties (27 MJ/kg) compared to bioethanol. When alkoxymethyl furan is blended with conventional fossil fuel, octane number and stability of blended fuel are improved that reported in previous study (Mariscal et al., 2016). Meanwhile, 5-HMF also can be converted to biofuel

by various ways. Dimethylfuran (DMF) has high potential as a high performance biofuel, and DMF can be obtained from hydrogenolysis reaction of 5-HMF (Roman-Leshkov et al., 2007). 5-Ethoxymethylfurfural (EMF) is also potential biofuel and obtained from catalytic reaction of 5-HMF with ethanol (Lew et al., 2012). Especially, compared to bioethanol, EMF gets attention due to its better fuel properties (8.7 kWh/l) and it can be directly applied to conventional gasoline engine without any modification (Alipour et al., 2017).

Consequently, it is important to utilize furan compound to high quality biofuel for overcoming current problems that originated from drawbacks of bioethanol usage such as low energy density and instability. As mentioned previously, furan compounds can be produced in integrated biorefinery as a promising precursor through chemical pretreatment. Therefore, improvement of integrated biorefinery is required for enhancing productivity of value-added furan compounds with obtaining economic feasibility.

1.4. Objectives

Currently, demand for alternative biofuel has increased since fossil fuel has faced environmental problem and crisis of depletion. However, bioethanol, the most widely used type of bioenergy, has inherent limitation due to low energy density. Therefore, development of biofuel has been studied which is applicable directly conventional system for petroleum utilization based transportation engine. Furthermore, high energy density biofuel development can be achieved through condensation reaction of furan derivatives with alcohol.

In this study, glucose and xylose which are abundant sugar will be degraded in organic solvents with solid catalyst, and their furan derivatives from glucose and xylose will be reacted to condense with organic solvents at the same time. And then, yield of furan derivatives will be analyzed by gas chromatography equipped with mass spectrometry and high performance liquid chromatography. Based on these results, key factors that influence on yield of furan derivatives will be evaluated. Finally, optimum condition for production of furan based biofuel will be determined.

Specifically, the aims of this study are;

1. To evaluate the conversion rate of glucose and xylose to furan derivatives and the yield of condensation products that can be used as a biofuel.
2. To analyze relationship between yield of condensation products and reaction condition for finding the key factors concerning about condensation reaction.
3. To determine optimum condition for production of furan based biofuel will be determined.

2. Literature reviews

2.1. EMF production from various feedstocks

Ethoxymethyl furfural (EMF) is produced by different starting materials such as 5-HMF, fructose, and glucose. Herein, EMF production process will be explained depending on starting materials, catalyst usages, and reaction condition.

2.1.1. 5-HMF to EMF conversion

EMF conversion from 5-HMF has been investigated with various reaction condition and catalysts such as homogenous mineral acids, ion exchange resin, zeolite, and etc in order to establish optimum reaction conditions (Alipour et al., 2017). Various catalysts are used. Even though homogeneous mineral acids performed excellent activities due to their high accessibility, separation and recycle process required considerable energy and time. Alternatively, solid acid catalysts can overcome those problem because easy product purification and catalysts recycling (Lanzafame et al., 2011). For these reason, many researchers have discovered to proper solid acid catalysts and modified the catalysts for improving their activities. Reaction temperature and reaction time were various from 70 to 140 °C, and from 2 to 24 h, respectively. Major byproduct of 5-HMF to EMF etherification reaction is ethyl levulinate (EL), and minor byproducts are 5,5'(oxy(methylene))bis-2furfural (OBMF) and 5-(ethoxymethyl)-furfural diethylacetal (EMFDEA) (Lanzafame et al., 2015). Liu et al achieved 92.9% of EMF yield from 5-HMF with Lewis acid catalyst AlCl_3 , with 100 °C of reaction temperature and 5 h of reaction time (Liu et al., 2013b). Balakrishnan et al. achieved 81% of EMF yield from 5-HMF using sulfuric acid as a Brønsted acid with 75 °C of reaction temperature 24 h of

reaction time. When Brønsted acid is used for 5-HMF etherification, significant EMFDEA can be produced at lower reaction temperature due to competition between acetalization and etherification using 5-HMF (Balakrishnan et al., 2012; Sacia et al., 2014). Compared to homogenous mineral acids, activities of zeolite are lower in EMF conversion. Lanzafame et al. conducted 5-HMF etherification using SBA-15, zirconia over SBA-15 and sulfated zirconia-SBA-15 with 140 °C of reaction temperature 5 h of reaction time (Lanzafame et al., 2011). As a result, 76% and 62% of EMF yield were obtained by SBA-15 and sulfated zirconia-SBA-15, respectively. Meanwhile, 1,1-diethoxy ethane (DE) was found as a major product using SBA-15. In contrast, EL was produced as a major product by strong Brønsted acids sulfuric acid and Amberlyst 15. The previous studies suggested that presence of Lewis acids such as zirconia over SBA-15 and sulfated zirconia-SBA-15 are appropriate for EMF production, while Brønsted acid lead EL formation instead of EMF production (Lanzafame et al., 2011). However, opposite results also observed. Liu et al. conducted EMF production using cellulose sulfuric acid with reaction temperature at 100 °C for 10 h, performed excellent results as 84.4% of EMF yield (Liu et al., 2013a).

In summary, 5-HMF can be converted to EMF by Lewis and Brønsted acid as catalysts. However, Brønsted acid can also produce EL or EMFDEA instead of EMF when reaction condition becomes severe. Therefore, appropriate reaction condition need to be set for EMF production in case of Brønsted acid as an acid catalyst.

2.1.2. Fructose to EMF conversion

To produce EMF from fructose, dehydration for converting fructose to 5-HMF as a precursor for EMF is required. Several catalysts were adopted for one-pot conversion from fructose to EMF including fructose dehydration and 5-HMF etherification. Balakrishnan et al. successively converted fructose to EMF (70% of EMF yield) in one-pot reaction using sulfuric acid as a Brønsted acid catalyst, reaction temperature at 100 °C for 24 h (Balakrishnan et al., 2012). Liu et al. converted fructose to EMF (71.2% of EMF yield) using AlCl₃ as a Lewis acid catalyst, reaction temperature at 100 °C for 11 h (Liu et al., 2013b).

Meanwhile, EMF yield is quite low when using zeolite from fructose. Li et al. used H-Y and H-beta at 96 °C for 11 h, yielding under 20% of EMF. The yield of EMF can increase when zeolite and Amberlyst 15 were adopted sequentially. And Li et al added H-USY zeolite for 5 h followed by Amberlyst 15 for another 6 h with same reaction condition previously, resulting in 67% of EMF yield (Li et al., 2016).

In short, at least two kind of catalysts are required when adopting zeolites as catalysts for conversion of fructose to EMF. In comparison 5-HMF, fructose to EMF conversion reaction needs to higher reaction temperature and longer reaction time for fructose dehydration (Alipour et al., 2017).

2.1.3. Glucose to EMF conversion

Compared to fructose and 5-HMF, overall yield of EMF from glucose is relatively low because glucose to EMF conversion requires isomerization of glucose to fructose, dehydration of fructose to 5-HMF, and etherification of 5-HMF (Figure. 2). Nevertheless, glucose is favorable feedstock because it is the most abundant and the cheapest monosaccharide. Many researchers tried

to convert glucose to EMF in one-pot system for saving the purification cost. Yang et al. converted glucose to EMF using $\text{AlCl}_3 \cdot 6\text{H}_2\text{O}$ with reaction temperature 160°C for 15 min (Yang et al., 2012). Although EMF yield was 33%, it is noteworthy because it produced EMF in short time compared with other reactions. Zeolite was also used for EMF production from glucose. Lew et al. conducted glucose conversion to EMF using tin-beta zeolite and Amberlyst 131 with reaction temperature 90°C for 24 h, resulting in 31% of EMF yield (Lew et al., 2012). Li et al. also use zeolite with various acid catalysts such as Amberlyst 15, SBA-15- SO_3H , Nafion NR50, and etc. Among them, tin-beta zeolite with Amberlyst 15 (reaction temperature: 96°C , reaction time: 11 h) showed good performance by 43% of EMF yield (Li et al., 2016).

To sum up, glucose to EMF conversion shows low EMF yield compared to 5-HMF or fructose. And glucose to EMF conversion commonly requires long reaction time in mild temperature for preventing further degradation of EMF to ethyl levulinate as reaction starting from 5-HMF or fructose mentioned previously. However, there is possibility to EMF production from glucose with relatively high reaction temperature and short reaction time (Yang et al., 2012). Therefore, it is quite interesting to enhance EMF production under high temperature with short reaction time.

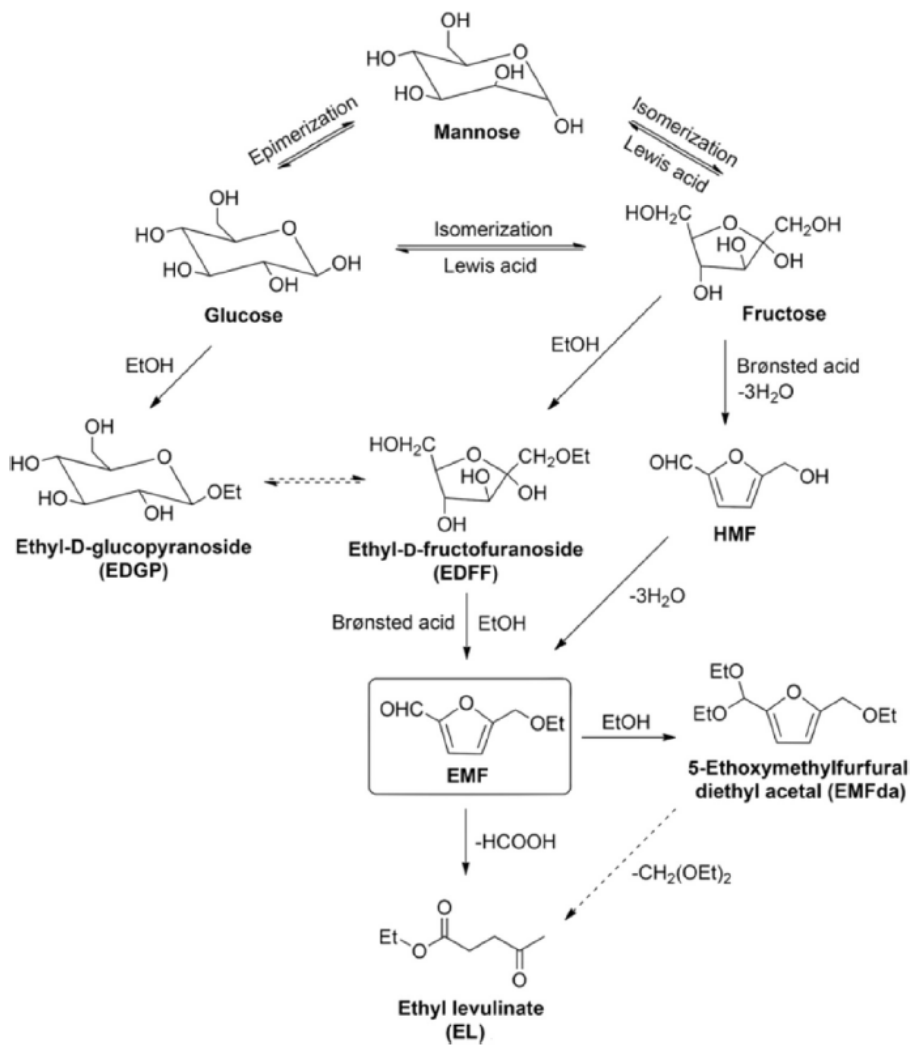


Figure 2. Proposed reaction mechanism from glucose to EMF (Li et al., 2016).

2.2. Alkoxymethyl furan production from various feedstocks

Alkoxyethyl furan is usually converted from furfuryl alcohol through simple etherification catalyzed by acid catalyst (Bui et al., 2013). Recently, researchers tried to alkoxyethyl furan from furfural because furfural can be easily produced by C5 pentose sugar such as xylose using acid catalyst during thermal reaction. Herein, alkoxyethyl furan production process will be explained depending on starting materials, catalysts, and reaction condition.

2.2.1 Furfuryl alcohol to alkoxyethyl furan conversion

Alkoxyethyl furan conversion from furfuryl alcohol is commonly preferred with mild acidic catalyst such as zeolites (Antunes et al., 2015). Furfuryl alcohol was reacted with ethanol using ZSM-5 zeolite with reaction temperature 125 °C for 2.5 h, and maximum yield of alkoxyethyl furan was 50 mol% with under 10 mol% of EL, lactic acid, and angelica lactone as byproducts (Mariscal et al., 2016).

2.2.2. Furfural to alkoxyethyl furan conversion

Alkoxyethyl furan from furfural can be divided two steps. Furfural is hydrogenated to furfuryl alcohol followed by etherification. Because furfural has high vapor pressure, furfuryl alcohol from can be produced by two ways: gas phase and liquid phase reaction (Jae et al., 2014). Gas phase reaction was first reported in 1929 using Cu as a catalyst (Mariscal et al., 2016). Since then, various catalysts such as Cu/SiO₂, Cu/SBA-15, PdCu/zeolite-Y, and etc. were used for furfuryl alcohol production in gas phase (Mariscal et al., 2016; Seo & Chon, 1981; Vargas-Hernandez et al., 2014). Meanwhile, furfuryl alcohol production in liquid phase mainly affected by solvent type. Aqueous solvents

typically produce cyclopentanol or cyclopentanone, while organic solvents produce furfuryl alcohol, tetrahydrofurfuryl alcohol, and methyl furan (Horvath et al., 2013; Hronec et al., 2012; Ordonsky et al., 2013). Catalysts used in liquid phase reaction are various, such as Ru/C, Pt/C, Fe-Ni-B, Co-Ni-B. n-butanol, ethanol, and methyltetrahydrofuran are used as solvents (Hronec et al., 2012; Li et al., 2003; Liaw et al., 2008; Ordonsky et al., 2013).

However, use of hydrogen during alkoxyethyl furan conversion led to several problems such as unsafety, high compression cost, difficulty of transportation, and stability for storage (Gandarias et al., 2013; Gandarias et al., 2012). To overcome these problems, alternative ways to supply hydrogen without hydrogen gas are required. Transfer hydrogenation is one of these ways that can provide hydrogen molecule derived from hydrogen donor (Panagiotopoulou & Vlachos, 2014). Alcohols get attention as a hydrogen donor because of their safety, high regeneration ability. Moreover, alcohols can serve as solvents and reactant simultaneously (Bui et al., 2013; Chia & Dumesic, 2011; Jae et al., 2013). Meerwein-Ponndorf-Verley (MPV) reduction is one of the transfer hydrogenation that reduce ketone or aldehyde to alcohol. Furfural can be converted to furfuryl alcohol via MPV reduction process with reduction of carbonyl group in the furfural. Lewis acid can act as a catalyst in MPV reduction and catalyze to alcohol etherification (Jae et al., 2014; Lewis et al., 2014). According to the previous study, alkoxyethyl furan can be converted from furfural in one-pot conversion. Bui et al. produced alkoxyethyl furan and furfuryl alcohol using zirconia –beta and 2-butanol as a solvent with reaction temperature 120°C for 0.08 h (Bui et al., 2013). It is notable that furfural can be converted to alkoxyethyl furan in short time by single Lewis acid catalyst such as zirconia-beta. Koehle and Lobo produced alkoxyethyl furan using tina-beta zeolite and 2-propanol as a solvent with reaction temperature 135°C for 250 min. They also tested hafnium-beta and

zirconia-beta at the same reaction condition, resulting in high furfuryl alcohol selectivity instead of alkoxyethyl furan (Koehle & Lobo, 2016). Interestingly, the yield of alkoxyethyl furan can be changed depending on solvent in previous studies. 58% of alkoxyethyl furan was produced from furfural when solvent was 2-butanol (reaction temperature: 120 °C, reaction time: 5 h), while 7% of alkoxyethyl furan was observed using 2-propanol as a solvent (Antunes et al., 2015). To estimate effect of solvents for furfural conversion to furfuryl alcohol or alkoxyethyl furan, various alcohol such as ethanol, 1, 2-propanol, 1, 2-butanol, and 2-pentanol were tested. As a results, secondary alcohols were effective in transfer hydrogenation due to its low solvent polarity (Panagiotopoulou et al., 2014). On the other hand, etherification of furfuryl alcohol with solvent (alcohol) was enhanced as shortening of alcohol chain by steric effect (Panagiotopoulou et al., 2014). Furfural conversion reaction with alcohol solvent using acid catalyst produces various products including alkoxyethyl furan (Figure 3). 2-methyl furan can be produced via reduction of furfuryl alcohol (Panagiotopoulou & Vlachos, 2014), while alkyl levulinate can be also produced via hydrolysis of alkoxyethyl furan (Hernandez et al., 2016). Therefore, appropriate reaction condition, solvent, and catalyst are needed to improve alkoxyethyl furan production.

2.2.3. Xylose to alkoxyethyl furan conversion

Xylose is a major component in hemicellulose, and easily obtained because hemicellulose is readily degraded during acid hydrolysis in integrated

biorefinery (Octave & Thomas, 2009). For this reason, xylose is considered as one of the main precursors of furan compounds (Carrasquillo-Flores et al., 2013).

There are some researches for alkoxyethyl furan from xylose in one-pot conversion. Hernández et al. conducted γ -valerolactone production from xylose in one-pot conversion using zirconia-aluminium-beta zeolite with 2-propanol as a solvent. As a result of previous study, alkoxyethyl furan was produced as a byproduct but the amount was trace (Hernandez et al., 2016). There are some reasons to prevent one-pot conversion from xylose to alkoxyethyl furan. First, xylose can be converted to xylitol or lactate by Lewis acid catalyzed reaction in alcohol, resulting in low furfural conversion rate (Holm et al., 2010; Yi & Zhang, 2012). Second, furfural is relatively cheap among the furan compound (1000-1450 \$/t) therefore it is more convenient to use furfural instead of xylose (Mariscal et al., 2016). Although xylose has some bundles to be converted to alkoxyethyl furan in one-pot conversion, it will be worthy if one-pot conversion of xylose to alkoxyethyl furan because of saving cost for purification.

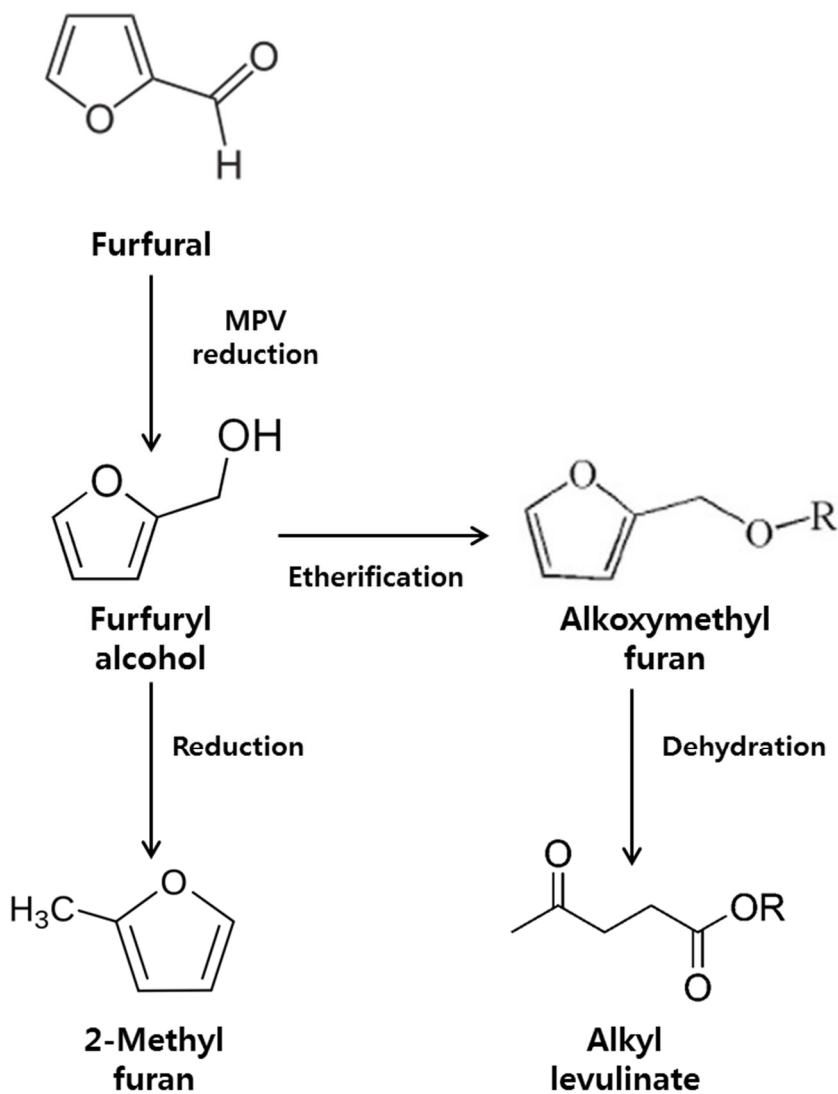


Figure 3. Proposed reaction pathway of furfural conversion by acid catalyst.

2.3. Acidic properties of zeolite

2.3.1. Lewis and Brønsted acidity on zeolite

Zeolite is catalytic material which has porous crystalline structure, consisting of Si, Al, and O atoms (Niwa et al., 2010). Although structure and pore design of zeolites are various, acidic sites expressed by zeolite are similar (Roy et al., 2013).

Brønsted acidic properties are mainly affected by hydrogen bond with the oxygen atom which is connected to tetrahedrally coordinated cations in zeolite frame. In acidic condition, proton can be connected with zeolite framework and role as an acid catalyst. There are four bridging OH group depending on structure of surrounding cations: $\text{Al}_3\text{Si-OH-AlSi}_3$, $\text{Al}_2\text{Si}_2\text{-OH-AlSi}_3$, $\text{AlSi}_2\text{Si-OH-AlSi}_3$, and $\text{Si}_3\text{Si-OH-AlSi}_3$ (Deka, 1998). The Brønsted acidity of zeolite is determined by electronegativity of surrounding atoms. When electronegativity of surrounding atoms is strong, electron is shifted from H to O followed by weakening of hydrogen bond (Gutmann, 1978). Consequently, proton is released from weaken hydrogen bond and leads to strengthen acidity. Lewis acidic properties are exhibited by electron deficient sites such as added cationic sites, M^{n+} , AlO^+ or $\text{Al}_x\text{O}_y^{n+}$ clusters on inside or outside of the pores. As shown in Figure 4. These aluminium clusters are formed by pretreatment, activation, and dehydration of zeolite (Kondo et al., 2010).

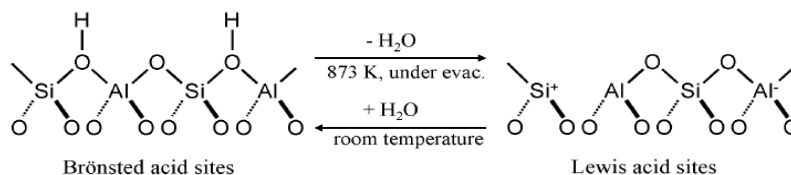


Figure 4. Exhibition of Lewis acid sites on zeolite. (Kondo et al., 2010).

2.3.2. Zeolite modification

Although zeolites itself can act as catalysts, zeolites are modified to enhance acidic properties depending on substrates. Dealumination and metal

impregnation are widely used modification methods because of their simple process and remarkable property changes (Dijkmans et al., 2013; Heinichen & Holderich, 1999). Dealumination process includes impregnation in strong acidic solution such as nitric acid or hydrochloric acid and rate of dealumination can be controlled by concentration of acidic solution (Maache et al., 1993). By dealumination process, aluminium clusters or OH group bridging are diminished followed by decrease of acidities (Roberge et al., 2002). Metal impregnation in zeolite generally gives rise to improvement of Lewis acidity due to adding cations (Moreno-Recio et al., 2016). Even though same amount of metal cations are impregnated, Lewis acidity can be different depending on kind of metal cations. It is known that absolute electronegativity which is generally considered as average of ionization energy and electron affinity correlates with Lewis acidity (Li et al., 2015). However, exact role of metal for various Lewis acid catalyzed reaction is not clear. For example, tin-beta showed high activity for glucose isomerization, while zirconium or hafnium-beta showed high activity for MPV reduction (Koehle & Lobo, 2016). Therefore, appropriate metal impregnation of zeolites is necessary for establishing optimum condition of chemical reaction.

3. Materials and methods

3.1. Materials

Glucose and xylose (purity: > 99%), which are most abundant monosaccharides in lignocellulosic biomass, were selected as standard materials and purchased from Sigma Aldrich Korea Co. (Yongin, South Korea). Ethyl levulinate, furfural, and 5-HMF (purity: 99%) which are standard materials for quantitative analysis were also purchased from Sigma Aldrich Korea Co. And decane (purity: 98%) for internal standard in gas chromatography was purchased from SAMCHUN chemical (Pyeongtaek, South Korea).

3.2. Catalyst preparation

Solid acid catalysts used in alcoholysis are Amberlyst 15, and zeolite beta (CP 814C, Si/Al=38, cation form: ammonium). Amberlyst 15 which is known as sulfonic acid resin (dry, hydrogen form) was purchased from Sigma Aldrich Korea Co. and zeolite beta was purchased from Zeolyst International (PA, USA). Tin(IV) chloride pentahydrate ($\text{SnCl}_4 \cdot 5\text{H}_2\text{O}$, purity: 98%), nitric acid (assay: 60%), and 2-propanol (purity: 99.5%) used for zeolite modification were purchased from SAMCHUN chemical.

3.2.1. Zeolite modification

Zeolite was modified to increase its Lewis acidity by following methods. Zeolite beta was denoted as NH_4 -BEA, and NH_4 -BEA dealuminated by 7 M of nitric acid for overnight (zeolite:nitric acid solution= 1:20 (w/v)), and washed by deionized water and filtered. Dealuminated NH_4 -BEA (denoted as DeAl-BEA) then treated by 135 mmol of $\text{SnCl}_4 \cdot 5\text{H}_2\text{O}$ in 2-propanol (zeolite: $\text{SnCl}_4 \cdot 5\text{H}_2\text{O}$ solution=1:100 (w/v)) for 7 h under reflux condition. After Sn metal impregnation, modified zeolite was washed, filtered by 2-propanol and

dried. Then zeolite was calcinated. Calcination procedure was as followed. First, zeolite was heated to 200°C by heating rate of 3°C/min. Then dwelled for 6 h and heated to 550°C by heating rate of 3°C/min. finally, zeolite dwelled for 6 h. Modified zeolite was denoted as Sn-BEA.

3.3. Catalyst properties analysis

3.3.1. BET surface area and pore volume analysis

The surface area of the zeolite was determined by nitrogen adsorption desorption using ASAP 2010 (Micromeritics, USA) apparatus. Pore volume distribution was analyzed from desorption isotherms by BJH (Barret-Joyner-Halenda) method using the Halsey equation for multilayer thickness. Total pore volume was taken at $p/p_0=0.975$ of a single point.

3.3.2. Powder X-ray diffraction (XRD) analysis

XRD pattern analysis for zeolite was conducted using D8 Advance with Davinci equipped with Lynxeye XE as a detector (Bruker, Germany). 2θ range was 5-70 degree (step: 0.02, scan speed: 0.5 sec/step, Cu $K\alpha$ radiation) and wavelength was (λ) was 1.5418Å.

3.3.3. Wavelength dispersive X-ray fluorescence (WDXRF) analysis

WDXRF spectrometry for aluminum and silica ratio analysis was conducted by S8 tiger (Bruker, Germany). Sample mask for cutting unwanted signal was

34 mm, and gas for analysis of powder was helium.

3.3.4. Temperature-programmed desorption (TPD) analysis

Acidic properties of solid acid catalysts were measured by Temperature-Programmed Desorption measurement of NH_3 (NH_3 -TPD). 100 mg of catalysts were loaded into TPD apparatus (Belcat II, MicrotracBEL Corp., Japan). Catalysts were pretreated by following sequence: In helium atmosphere (flow rate: 50 ml/min), catalysts were heated to 200 °C and maintained for 50 min to remove organics on catalysts. Then catalysts were cooled to 50 °C and NH_3 was attached to catalysts (8.5% NH_3/He , flow rate: 50 ml/min) for 30 min. After that, catalysts were heated to 150 °C to desorb physically attached NH_3 on catalysts and cooled to 50 °C in helium atmosphere (flow rate: 50 ml/min).

Desorption of chemically bonded NH_3 on acid site of catalysts was conducted from 150 to 650 °C with 10 °C/min of heating rate in helium atmosphere (flow rate: 30 ml/min). Desorbed NH_3 was determined by thermal conductivity detector (TCD).

3.4. Reaction studies

3.4.1. One-pot conversion of glucose to EMF

One-pot conversion of glucose to EMF was conducted in stainless batch-type reactor (Bolted Closure Vessels, Hanwoul Engineering, Gunpo, South Korea). 0.1 g of glucose and 0.05 g of solid catalysts (Sn-BEA+Amberlyst 15) were loaded into glass reactor. Then 4 ml of ethanol was poured into reactor and final solid:liquid ratio (w/v) was 1:40. Amberlyst 15:Sn-BEA ratio (w/w) was set as 0:1, 1:0, 1:1. Reactor was heated to reach the desired temperature (180, 190, 200 °C) in 50 min and maintained the reaction temperature for 10, 20, and 30 min. After reaction, reactor was cooled to room temperature by the ice chamber. Liquid fraction after reaction were collected and filtered through 0.45 µm membrane filter (Advantec Co., Tokyo, Japan) for sugar and sugar derivatives (furan compound, organic acid and derivatives, etc) analysis. And Sn-BEA after reaction were collected, washed, and calcinated at 550 °C for reusability test.

3.4.2. Glucose to EMF conversion reaction by changing solid catalyst ratio

When optimum condition for EMF production was confirmed at previous reaction results, Amberlyst 15:Sn-BEA ratio (w/w) was changed to determine effect of type of acidity on EMF conversion reaction. As 0.025 g of Amberlyst 15, amount of Sn-BEA was set 0.0125, and 0.05 g for changing Lewis acidity. Then procedure was conducted again as 0.025 g of Sn-BEA with 0.0125, and 0.05 g of Amberlyst 15 for Brønsted acidity. Liquid fraction analysis was proceed same as mentioned in section 3.4.1.

3.4.3. Furfural to alkoxyethyl furan conversion reaction

Conversion of furfural to alkoxyethyl furan reaction to estimate Lewis acid catalyzed MPV reduction and etherification was conducted by stainless batch-

type reactor. 0.1 g of furfural with 0.05 g of Sn-BEA loaded into glass reactor. Then, 4 ml of 2-propanol was poured into reactor and final liquid:liquid ratio (w/v) was 1:40. Reaction temperature was 170, 180, and 190°C, and reaction time was set as 10 min. After reaction, same procedures were conducted as glucose conversion reaction mentioned in section 3.4.1.

3.4.4. One-pot conversion of xylose to alkoxyethyl furan

One-pot conversion of glucose to EMF was conducted in stainless batch-type reactor. 0.1 g of xylose and 0.05 g of solid catalysts (Sn-BEA+Amberlyst 15) loaded into glass reactor. Then 4 ml of 2-propanol was poured into reactor and final solid:liquid ratio (w/v) was 1:40. Amberlyst 15:Sn-BEA ratio (w/w) was set as 0:1, 1:0, 1:1. Reactor was heated to reach the desired temperature (170, 180, 190°C) in 50 min and maintained for 10 min. After reaction, same procedures were conducted as glucose conversion reaction mentioned in section 3.4.1.

3.4.5. Zeolite reusability test

Sn-BEA reusability test was performed by comparison of alkoxyethyl furan yield starting from furfural. Same reactor mentioned previously was used in this reaction, 0.1 g of furfural and 0.05 g of Sn-BEA loaded into glass reactor. Then 4 ml of 2-propanol was poured into reactor and final liquid:liquid ratio (w/v) was 1:40. Reaction temperature was 190°C and reaction time was set as 10 min. After reaction, same procedures were conducted as furfural to alkoxyethyl furan conversion reaction mentioned in section 3.4.3.

3.5. Analysis of liquid fraction

3.5.1. Analysis of liquid fraction of glucose conversion reaction

The concentration of sugars and 5-HMF, EMF after reaction were determined by high performance liquid chromatograph (Ultimate-3000, Thermo Dionex, CA, USA) with a Aminex 87H column (eluent: 0.01 N sulfuric acid, oven temp: 40 °C, flow rate: 0.5 ml/min, injection volume: 10 µl). Calibration curves were obtained by standard solution. Peaks were identified by retention time and quantification of each compounds were identified by comparison with standard peak areas. EL was determined by gas chromatography equipped with mass spectrometry (gas chromatography: 7890B, CA, USA, mass spectrometry: 5977A, CA, USA). The stationary phase of gas chromatography was a DB-5ms capillary column (30 m × 250 µm ID × 0.25 µm coating thickness). Temperature of injector and detector are 250 °C and 300 °C, with split ratio of 7.5:1. The column temperature increases from 40 to 100 °C at a heating rate of 2.5 °C/min, and helium was used as a carrier gas (flow rate: 2 ml/min). Peak identification was based on comparison of mass spectra with the National Institute of Standard and Technology (NIST) library. Concentration EL was measured by internal standard (decane) considering response factors between furan derivatives and internal standard.

3.5.2. Analysis of liquid fraction of furfural and xylose conversion reaction

The concentration of sugars and sugar alcohol after reaction were determined by bio-liquid chromatography (ICS-2500, Thermo Dionex, CA, USA) equipped with CarboPac PA-1 column (250 × 4 mm) and pulsed amperometry detector (HP 1100, Hewlett Packard, CA, USA). KOH was used as a eluent (flow rate: 1 ml/min) and concentration of eluent versus time was as followed: 1-36 min: 2 mM, 35-36 min: 100 mM, 36-56 min: 100 nM, 56-63 min: 2 mM. Peaks were identified by retention time and quantification of each compounds were identified by comparison with standard peak areas. The concentration of furan derivatives were determined by gas chromatograph equipped with mass spectrometry as described in section 3.5.1.

4. Results and discussions

4.1. Physicochemical properties of zeolites

XRD patterns of zeolites are measured for indicating changes of crystalline structure by dealumination process (Figure 5). NH₄-BEA (Figure 5A) showed typical diffraction peaks corresponded with previous research (Akbar, 2010). And diffraction peaks of DeAl-BEA (Figure 5B) corresponded with peaks of NH₄-BEA. Contraction or expansion of zeolite matrix could be inferred by diffraction peak (302) at $2\theta=22.5-22.6^\circ$. Diffraction peak of NH₄-BEA and Sn-BEA presented at same $2\theta=22.64^\circ$, therefore d-spacing value were same (3.93 Å) (Baran et al., 2014). Based on these results, it seemed clearly that there was no significant crystalline structure change during zeolite dealumination process.

Table 1 showed the results of surface area, pore volume, and pore diameter of zeolites. Surface area of Sn-BEA increased compared to NH₄-BEA, due to removal of aluminium (Srivastava et al., 2009). On the other hand, pore volume, pore diameter increased slightly compared to surface area. It was assumed that mesopores distribution relatively remained by dealumination pores but micropores distribution were changed (Viswanadham & Kumar, 2006).

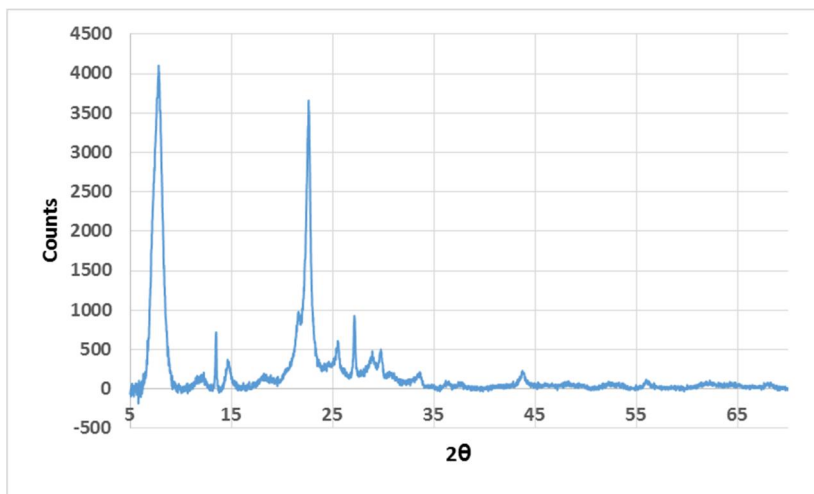
Table 1. Physicochemical properties of zeolites.

Catalyst	Surface area	Micropore area	Pore volume	Pore diameter	Si/Al ^a
----------	--------------	----------------	-------------	---------------	--------------------

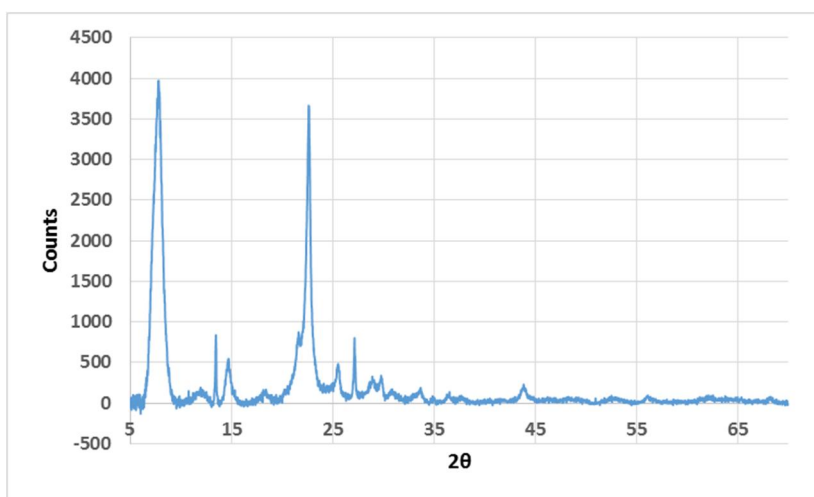
	(m ² /g)	(m ² /g)	(cm ³ /g)	(nm)	
NH ₄ -BEA	515.08	377.08	0.17	2.35	38 ^b
Sn-BEA	572.59	414.98	0.19	2.53	520

^a Measured by Wavelength dispersive X-ray fluorescence analysis

^b Referred by products MSDS



A



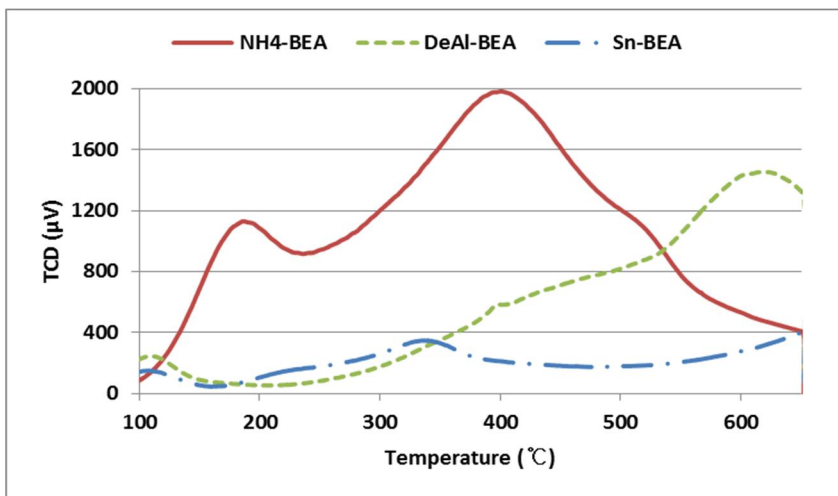
B

Figure 5. X-ray diffraction patterns of NH₄-BEA (A) and Sn-BEA (B).

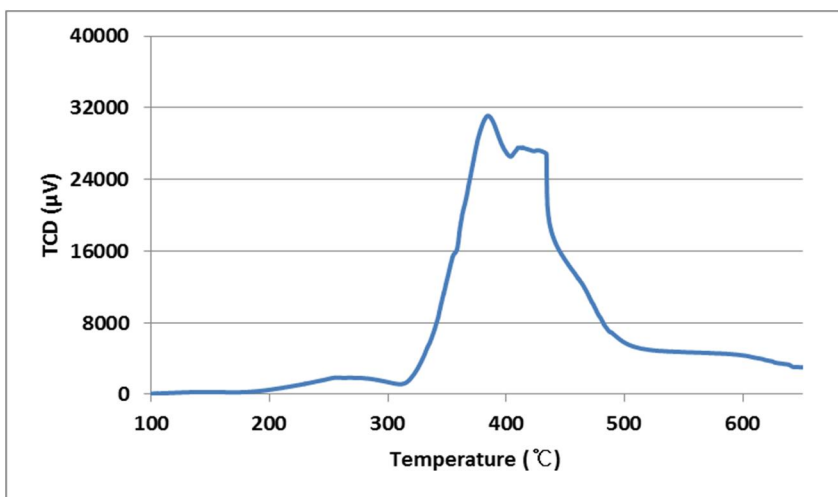
4.2. Acidic properties of solid acid catalysts

NH₃-TPD profiles showed acidic properties of zeolites (Figure 6A) and Amberlyst 15 (Figure 6B). In NH₄-BEA, major desorption occurred temperature at 180 and 380 °C. Considering that NH₃ desorbed at 180 °C indicated weak Brønsted acidity, temperature at 310 °C indicated moderate Brønsted acidity and temperature at 380 °C indicated strong Brønsted acidity (Nyalosaso et al., 2012), NH₄-BEA exhibited strong Brønsted acidity with moderated and weak one at the same time. On the other hand, after dealumination, peak existed at 180 °C disappeared, and peak at 380 °C was weakened. It meant that DeAl-BEA showed weak Brønsted acidity compared to NH₄-BEA. It assumed that during dealumination, SiOAl bridge which was exhibited strong Brønsted acidity disappeared (Yu et al., 2011). Sn-BEA exhibited weakest Brønsted acidity due to extra tin contents formed tin oxide (SnO) which is considered as base during metal impregnation (Marakatti & Halgeri, 2015). As a result, Brønsted acid site SiOAl bridge were decreased than DeAl-BEA.

NH₃-TPD profile of Amberlyst 15 was quite different with profile of zeolites. Amberlyst 15 showed high desorption peaks at 380 °C, which meant Amberlyst 15 had strong Brønsted acidity, but amount of NH₃ desorption was much larger than zeolite. Amberlyst 15 is sulfonic acid resins, therefore Amberlyst 15 had much more acidic sites compared to zeolite and these results were corresponded to previous research (Hodala et al., 2016).



A



B

Figure 6. NH₃-TPD profile of zeolites (A) and Amberlyst 15 (B).

4.3. One-pot conversion of glucose to EMF

4.3.1. EMF yield depending on reaction condition

Single catalyst such as Sn-BEA and Amberlyst 15 or Amberlyst 15+ Sn-BEA were used for evaluating how Brønsted or Lewis acid affected to glucose conversion to EMF. Figure 7, 8, and 9 Showed products distribution after reaction depending on reaction temperature and reaction time.

4.3.1.1. Reaction temperature at 180 °C

Figure 7 showed EMF and other products on reaction temperature at 180 °C with various catalysts and reaction time. When Sn-BEA with Amberlyst 15 (Figure 7A) was used, EMF yield was higher than that of single catalyst. Presence of Lewis acid isomerize glucose to fructose and accelerate 5-HMF production because 5-HMF dehydrated from 5 member monosaccharide ring such as fructose (Pagan-Torres et al., 2012). And Brønsted acid catalyze dehydration of fructose to 5-HMF. (Choudhary et al., 2013). For this reason, production of 5-HMF which is precursor of EMF could be boost by adopting Sn-BEA (Lewis acid) Amberlyst 15 (Brønsted acid) simultaneously (Lew et al., 2012). EMF yield increased as reaction time from 10 to 20 min, reaching maximum yield of 27.64%, and slightly decreased at reaction time 30 min. It might be concerned about EL because yield of EL yield gradually increased as increase of reaction time. EL can derived from of EMF by degradation reaction, therefore prolonged reaction time resulted in degradation of EMF and formation of EL (Li et al., 2016). Meanwhile, amount of 5-HMF was relatively low less than approximately 7% and gradually decreased as reaction time was prolonged. Because EMF is etherification products of 5-HMF and in

addition, EL could also be produced by levulinic acid which is produced by subsequent reaction of furan ring opening reaction and etherification of 5-HMF. Therefore, decrease of 5-HMF could lead to increase of EMF and EL yield (Lanzafame et al., 2011). Glucose low than approximately 2% in all reaction time. That meant complete consumption of glucose during the reaction. EL yield correlated with reaction time, maximum yield at 30 of reaction time (12.55%). Increase of EL yield is related to decrease of EMF and 5-HMF, which are precursor of EL. In Brønsted acidic condition, extension of reaction time in relatively high reaction temperature leads to opening of furan ring in 5-HMF and EMF followed by forming EL (Neves et al., 2013). Therefore, it was assumed that prolonged reaction time might be decrease of EMF yield and increase of EL yield.

On the other hand, glucose contents were significantly higher using Amberlyst 15 than using Sn-BEA+Amberlyst 15 (Figure 7B). It was assumed that Lewis acid Sn-BEA and Brønsted acid Amberlyst 15 create synergy effect by isomerization of glucose to fructose and fructose dehydration to 5-HMF subsequently. Another evidence that revealed this synergic effect is 5-HMF contents. 5-HMF contents in Amberlyst 15 was almost 1% or less, it is due to difficulty of isomerization catalyzed by Brønsted acid solely (Balakrishnan et al., 2012; Lew et al., 2012). And there might be considerable ethyl glucopyranoside not detected in this research as a result of Brønsted catalyzed etherification of glucose (Hu et al., 2011). Nevertheless, EMF was produced by Brønsted acid catalyzed etherification and its contents increased as reaction time was prolonged, and reaching maximum yield of 12.85%. EL yield increased as reaction time prolonged, maximum yield at 30 min of reaction time 20.12%). In comparison with reaction using Sn-BEA with Amberlyst 15, only Brønsted acidic condition promotes more EL production from 5-HMF or EMF and decrease EMF yield (Barbera et al., 2015).

Reaction using Lewis acid Sn-BEA showed quite different

compared to reaction using combination of Lewis and Brønsted acid or Brønsted acid solely (Figure 7C). Main difference was yield of EMF, which was quite lower (less than 6%). It because Lewis acid could isomerize glucose to fructose, but dehydration of fructose to 5-HMF was weak (Lew et al., 2012). As a results of weak dehydration strength, 5-HMF contents also low (less than 3%) compared to 5-HMF. Glucose were rarely detected in all reaction time, it is assumed that glucose isomerized to fructose by Lewis acid or formed ethyl glucopyranoside which is etherification product of glucose (Hu et al., 2011; Saravanamurugan et al., 2013). Unlike reaction using Sn-BEA with Amberlyst 15 or Amberlyst 15, EL could not found in Sn-BEA (Lewis acid) catalyzed reaction. It is due to EL production from EMF or 5-HMF is mainly affected by Brønsted acid that catalyze furan ring opening by protonation of oxygen in furan ring (Barbera et al., 2015).

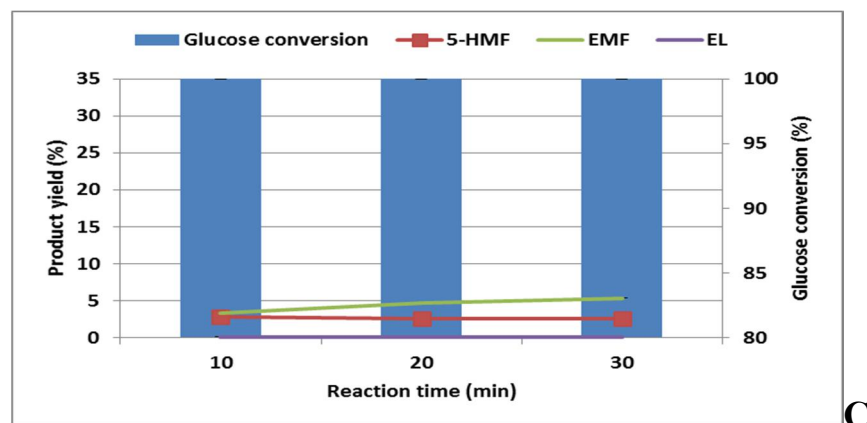
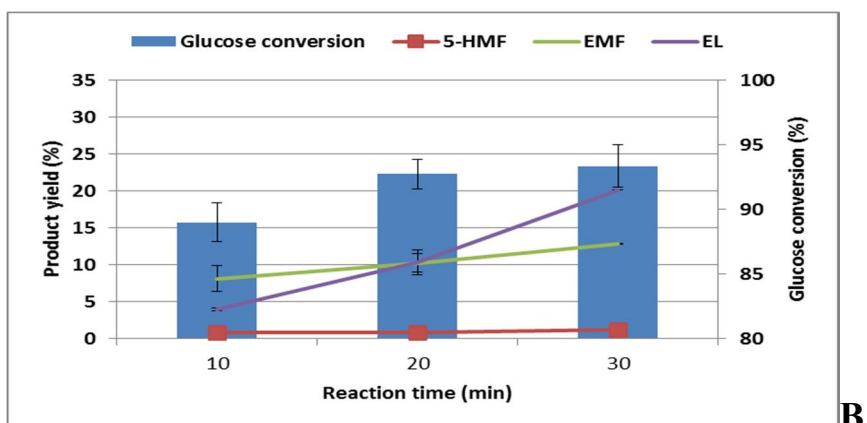
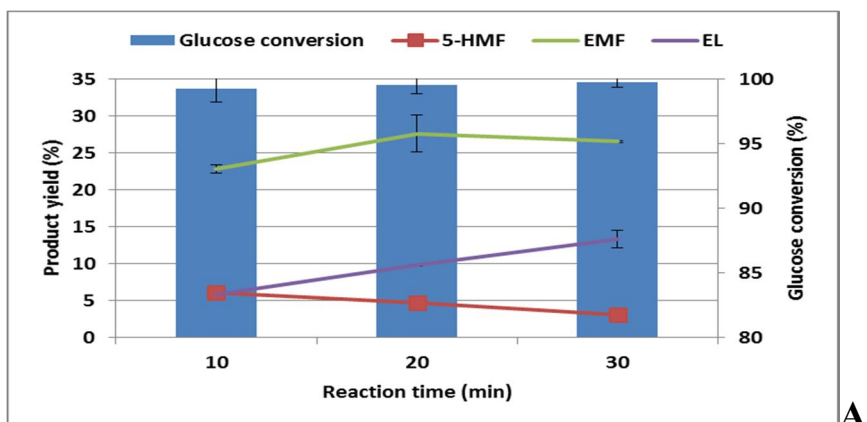


Figure 7. EMF yield at reaction temperature 180°C (A: Sn-BEA (0.025 g) with Amberlyst 15 (0.025 g), B: Amberlyst 15 (0.05 g), C: Sn-BEA (0.05 g))

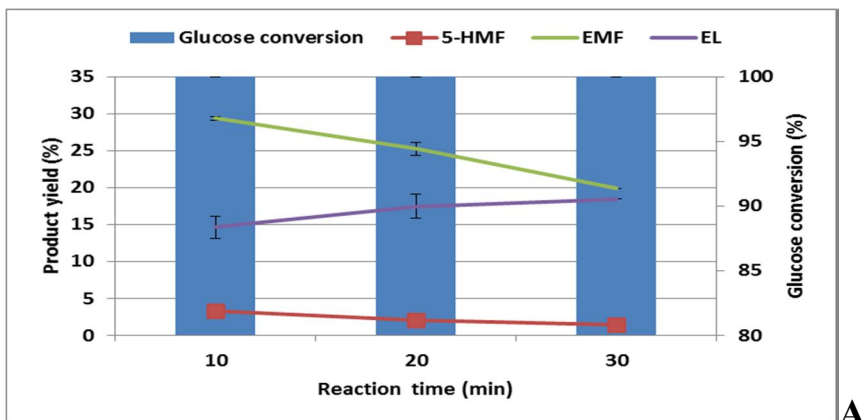
4.3.1.2. Reaction temperature at 190°C

Figure 8 showed EMF and other products contents on reaction temperature at 190°C. The trend of product distribution by catalyst uses or reaction time were similar with those of reaction temperature 180°C in section 4.3.1.1. In reaction catalyzed by Sn-BEA with Amberlyst 15 (Figure 8A), EMF yield reached maximum (29.37%) at reaction time 10 min, and decreased as reaction time was prolonged. It assumed that due to effect of high temperature, furan ring opened and decomposed to EL fast (Girisuta et al., 2006). 5-HMF contents were slightly lower than those of 180°C due to higher reaction temperature mentioned previously. EL were increased as reaction time was prolonged, reaching maximum yield (14.90%) at reaction time at 30 min. It was relatively high content in comparison with the result of reaction temperature at 180°C, indicating that frequency of furan ring opening reaction of EMF increased due to high temperature. Glucose contents was similar to those of reaction temperature at 180°C. EL yield was similar tendency with 180°C of reaction temperature using Sn-BEA with Amberlyst 15. EL yield increased as reaction time was prolonged, maximum yielded at 30 min of reaction time (18.45%).

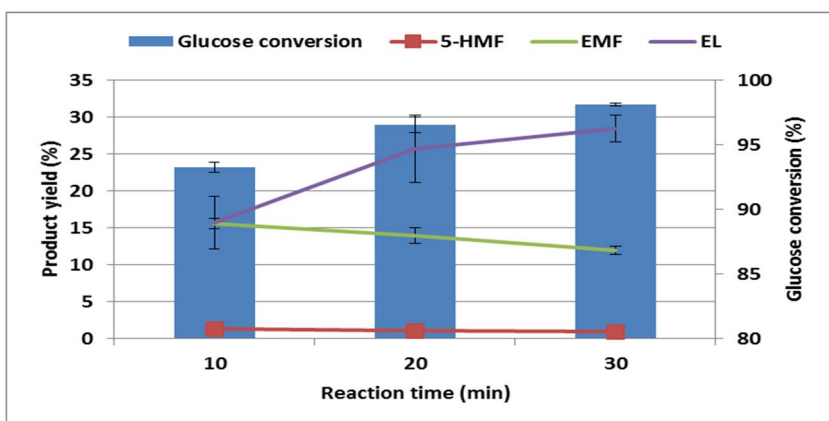
EMF yield using Amberlyst 15 (Figure 8B) were similar tendency with reaction using Sn-BEA+Amberlyst 15. EMF yield reached maximum (15.62%) at reaction time 10 min and decreased as reaction time went longer. It is caused by severe reaction condition compared to reaction temperature 180°C. At reaction temperature 190°C, EMF already reached maximum yield at reaction time 10 min and started to degrade (Girisuta et al., 2006). EL yield increased compared to 180°C of reaction temperature due to increase of reaction severity (Balakrishnan et al., 2012). As reaction time was prolonged,

EL yield increased and reached maximum (29.72%) at 30 min of reaction time.

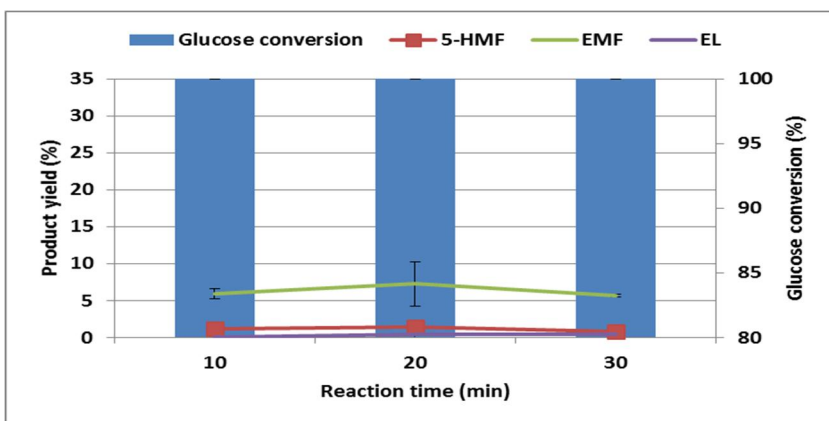
EMF yield using Sn-BEA (Figure 8C) remained constantly in all reaction time (approximately 6%). It seemed that EMF yield under Lewis acidic condition relatively because of low conversion rate of glucose to 5-HMF (Lew et al., 2012). EL yield was also low due to absence of Brønsted acid, as mentioned in section 4.3.1.1.



A



B

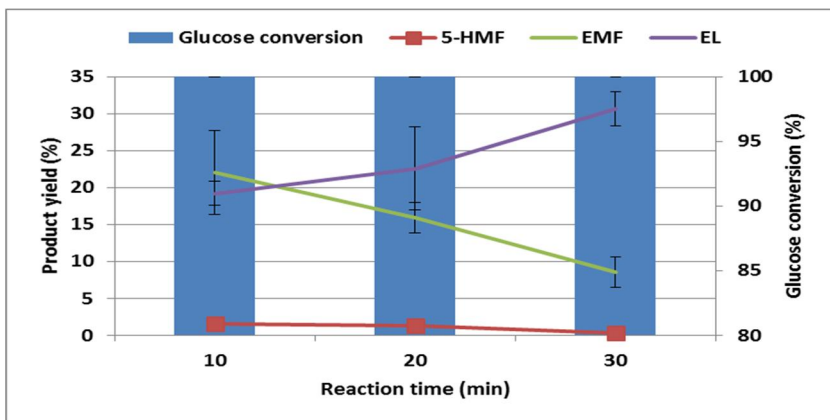


C

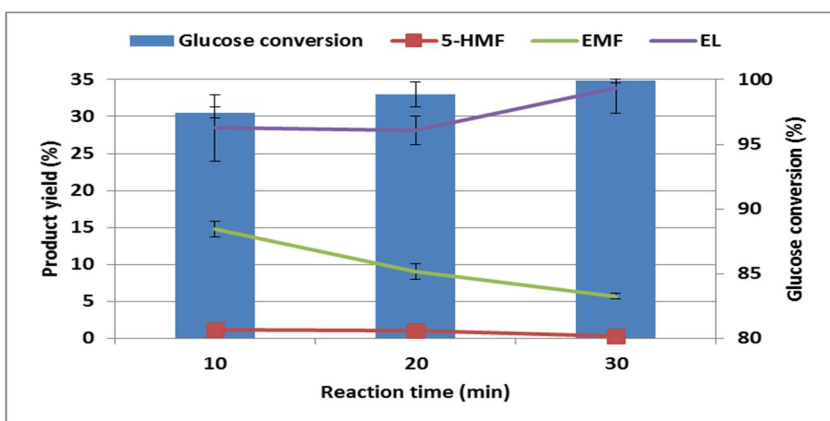
Figure 8. EMF yield at reaction temperature 190°C (A: Sn-BEA (0.025 g) with Amberlyst 15 (0.025 g), B: Amberlyst 15 (0.05 g), C: Sn-BEA (0.05 g))

4.3.1.3. Reaction temperature at 200 °C

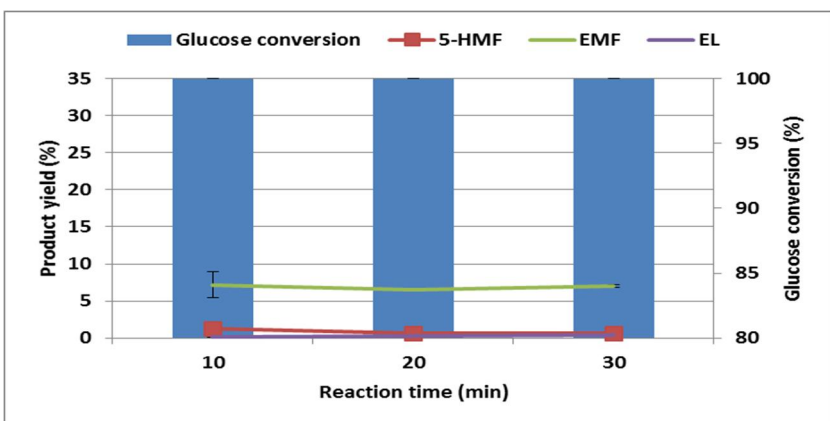
In case of Sn-BEA with Amberlyst 15 catalyzed reaction, EMF yield dropped more rapidly compared to reaction temperature at 190 °C (Figure 9A). On the contrary, EL yield sharply rose by increased reaction time from 20 to 30 min, maximum yield (32.28%) at 30 min of reaction time. It assumed that high reaction temperature and prolonged reaction time accelerates decomposition of EMF and production of EL (Girisuta et al., 2006). It is supported by Increase of EL yield and decrease of EMF yield. 5-HMF was almost decomposed regardless of reaction severity. Similar tendency also observed using Amberlyst 15 (Figure 9B), EMF yield dropped rapidly by increasing reaction time. 5-HMF, glucose were almost decomposed in all reaction time. In reaction using Sn-BEA, EMF contents slightly increased (approximately 7%) compared to reaction temperature at 190 °C (Figure 9C). Interestingly, reaction using Sn-BEA, EL yield was almost 0% even though its severe reaction condition. In addition, glucose was almost converted to other products. It is assumed that ethyl glucopyranoside which is produced by etherification of glucose or fructose produced by isomerization are still remained due to absence of Brønsted acid which catalyze dehydration reaction (Hu et al., 2011; Jeong et al., 2017).



A



B



C

Figure 9. EMF yield at reaction temperature 200°C (A: Sn-BEA (0.025 g) with Amberlyst 15 (0.025 g), B: Amberlyst 15 (0.05 g), C: Sn-BEA (0.05 g))

4.3.2. EMF yield depending on Lewis/Brønsted acid ratio

The highest yield of EMF accomplished at reaction temperature 190 °C, reaction time 10 min, and using Sn-BEA (0.025 g) with Amberlyst 15 (0.025 g) (29.37%). Lewis/Brønsted acid ratio was changed in this condition by giving variety to amount of Sn-BEA and Amberlyst 15. Figure 10 showed products distribution by changing Lewis/Brønsted acid ratio. When Lewis acidity was increased (Brønsted acid was fixed) (Figure 10A), EMF yield increased as weight ratio of Sn-BEA:Amberlyst 15 1:1 (Amberlyst 15, Sn-BEA: 0.025 g), EMF yield reached maximum (29.37%, same reaction condition at Figure 8A). And decreased as Amount of Sn-BEA was increased. It assumed that excessive Lewis acidic sites in reaction environment inhibited fructose which is isomerization product from glucose to 5-HMF dehydration, due to higher accessibility of fructose to Sn-BEA than Amberlyst 15 (Li et al., 2016). Similar tendency was observed in Brønsted acidity changed reaction (Figure 10B). As Brønsted acidity increased compared to Lewis acidity (Sn-BEA: 0.025 g, Amberlyst 15: 0.05 g), EMF converted EL due to higher strong Brønsted acidity by furan ring opening (Sacia et al., 2014). EL yield seemed to affected by Lewis/Brønsted acid ratio. When Brønsted acidity was dominant than Lewis acidity, reaction proceeded EMF to EL degradation. In contrast, when Lewis acidity was dominant, EL yield decrease but EMF yield also suppressed because of weak Brønsted acidity. Therefore, it was clear that catalyst ratio of 1:1 performed best because of appropriate balance of Lewis/Brønsted acidity.

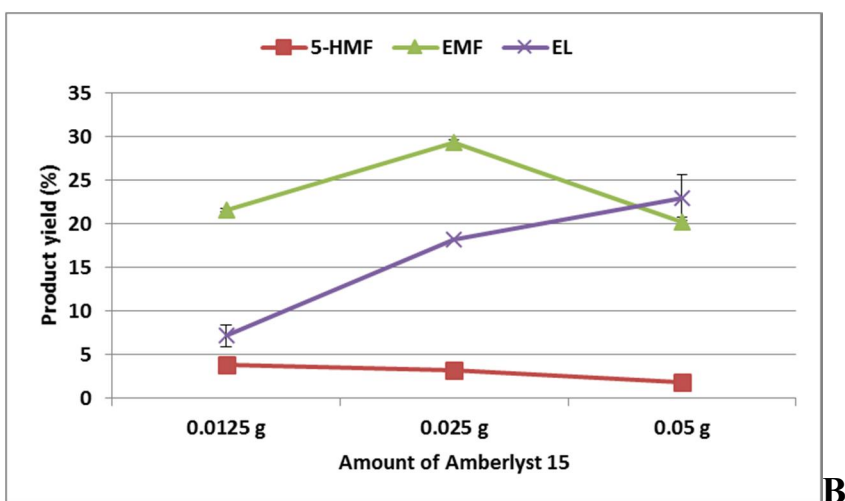
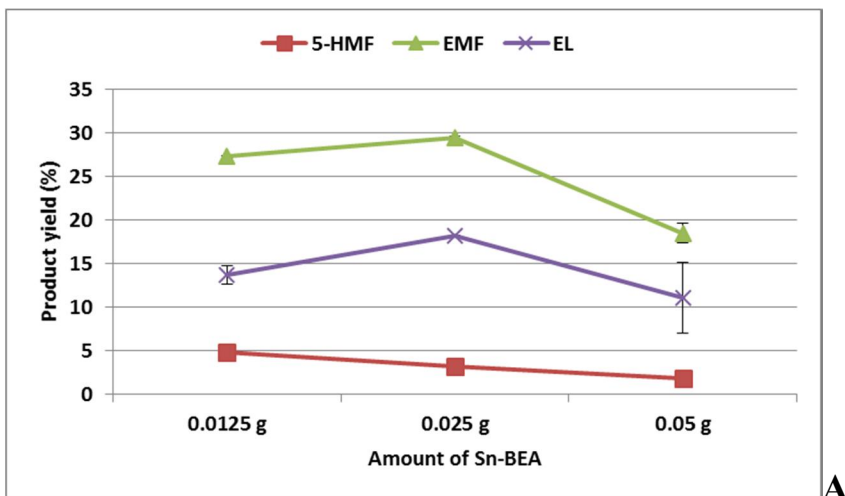


Figure 10. Glucose to EMF products distribution by changing Lewis/Brønsted acid ratio (reaction temperature: 190 °C, reaction time: 10 min). A: amount of Amberlyst 15 fixed as 0.025 g, B: amount of Sn-BEA fixed as 0.025 g

4.4. Conversion of furfural to alkoxyethyl furan

Contents of alkoxyethyl furan and furfural showed in Figure 11. In all reaction temperature, furfural converted to alkoxyethyl furan. Maximum alkoxyethyl furan yield from furfural was 36.73% at 190 °C of reaction temperature (reaction time: 10 min). By Lewis acid Sn-BEA, furfural reduced from furfuryl alcohol via MPV reduction by 2-propanol as a hydrogen donor (Gilkey et al., 2015). As temperature increased, furfural contents decreased while contents of alkoxyethyl furan increased. It seemed that Sn-BEA could transfer hydrogen from 2-propanol to furfural in short time (10 min). On the other hand, isopropyl levulinate also increased as reaction temperature increased. Generally, isopropyl levulinate was known for Brønsted acid catalyzed product from furfuryl alcohol or alkoxyethyl furan (Bui et al., 2013). Based on NH₃-TPD results, Sn-BEA processed weak Brønsted acidity with strong Lewis acidity and Lewis acid reduces activation energy in furfuryl alcohol or alkoxyethyl furan to isopropyl levulinate (Ahmad et al., 2016). Therefore, by assistance of Lewis acidity, weak Brønsted acidity in Sn-BEA could catalyze furfuryl alcohol or alkoxyethyl furan to isopropyl levulinate.

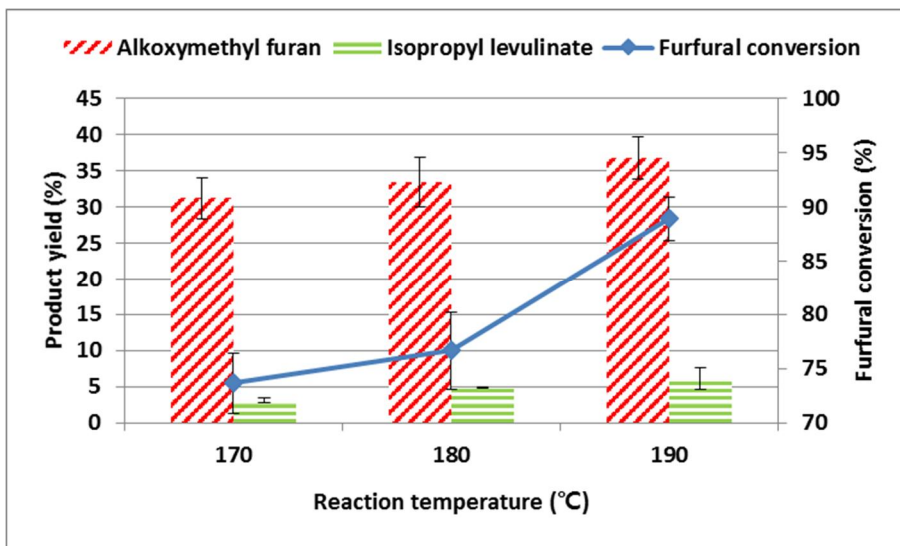


Figure 11. Contents of alkoxymethyl furan, and isopropyl levulinate after reaction of furfural conversion. (reaction time: 10 min, catalyst: Sn-BEA (0.05 g))

4.5. One-pot conversion of xylose to alkoxymerthyl furan

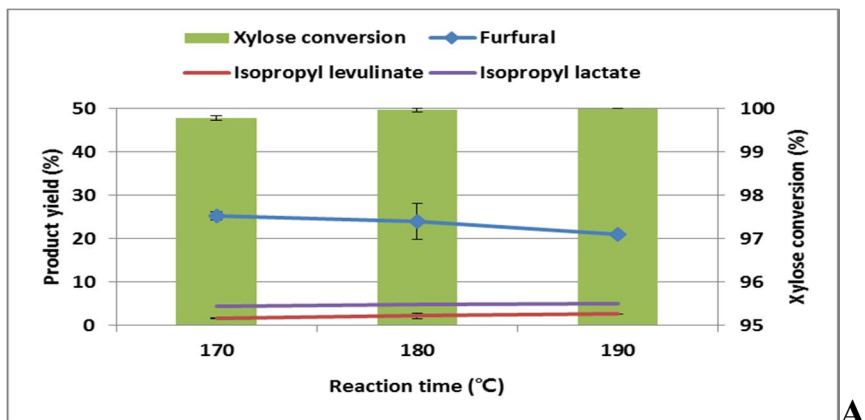
One-pot conversion from xylose to alkoxymerthyl furan was conducted by various catalysts and reaction temperature (Figure 12.). Unfortunately, there were no alkoxymerthyl furan conversion occurred in all reaction condition.

Xylose to furfural conversion successively by Amberlyst 15 (Figure 12A, B), while Sn-BEA showed poor furfural yield (Figure 12C) (less than 10%). Because xylose dehydration to furfural is mediated by Brønsted acid. Although Sn-BEA showed strong Lewis acidity than Brønsted acidity, Lewis acid could isomerize xylose to xylulose, and it reduces reaction energy from xylose to furfural (Ahmad et al., 2016). As a result, Sn-BEA could catalyze xylose to furfural with weak Brønsted acidity. However, this is still not enough to explain why furfural formed from xylose could not undergo MPV reduction via Sn-BEA even though xylitol which was possible inhibitor of alkoxymerthyl furan production produced by Lewis acid catalyzed reduction of xylose was not detected. One possible explanation is alkyl lactate formation catalyzed by Lewis acid. Isopropyl lactate was detected when Sn-BEA was used. In previous studies, lactate was produced from hexose such as glucose or fructose via retro-aldol reaction using Lewis acid (Taarning et al., 2011). Pentose such as xylose could be converted to lactate with Lewis acid but low lactate yield compared to hexose (Elliot et al., 2017). Isopropyl lactate produced only in presence of Lewis acid (Sn-BEA with Amberlyst 15, Sn-BEA). Especially, only Sn-BEA was used for catalyst, isopropyl lactate yield was similar with that of furfural. It was assumed that Sn-BEA catalyze xylose to isopropyl lactate instead of furfural to furfuryl alcohol. .

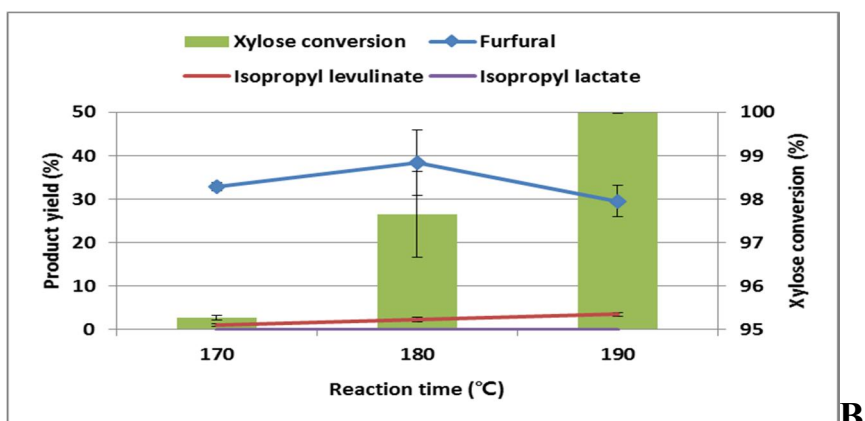
In Sn-BEA+Amberlyst 15 catalyzed reaction (Figure 12B), even though xylitol were not detected, furfural to alkoxymerthyl furan conversion was not

occurred. This might be Brønsted acid catalyzed dehydration reaction of 2-propanol to propylene, which inhibits zeolite activation by etherification with 2-propanol (Triantafyllidis & Evmiridis, 2000). Propylene formation was identified by gaseous formation after reaction when using Amberlyst 15 and presence of diisopropyl ether detected by gas chromatography.

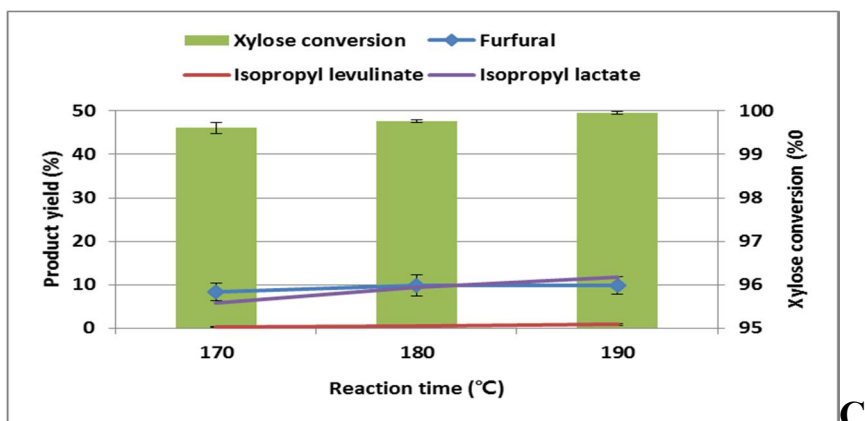
To overcome these problems, xylose to furfural production process and furfural to alkoxyethyl furan production process needs to be separated. Furfural yield need to be maximize by using appropriate Brønsted acid for dehydration of xylose to furfural and alkoxyethyl furan yield needs to be maximize by adopting suitable Lewis acid catalyst for MPV reduction and etherification.



A



B



C

Figure 12. Xylose to alkoxy methyl furan products distribution in 2-propanol (Reaction time: 10 min, A: Sn-BEA (0.025 g) with Amberlyst 15 (0.025 g), B: Amberlyst 15 (0.05g), C: Sn-BEA (0.05 g)).

4.6. Catalyst reusability

Figure 13 showed catalyst reusability from one to three times uses. Surprisingly, catalytic activity increased in two times reaction than one time reaction. It probably due to calcination process for diminishing organics attached at zeolite for reuse. During calcination, hydrogen bonds in SiOAl bridge was reduced and form new Lewis acidic sites (Kondo et al., 2010). Considering calcination effect on two time reaction, Sn-BEA activity remained constant until 2nd time uses and slightly decreased at 3rd time uses.

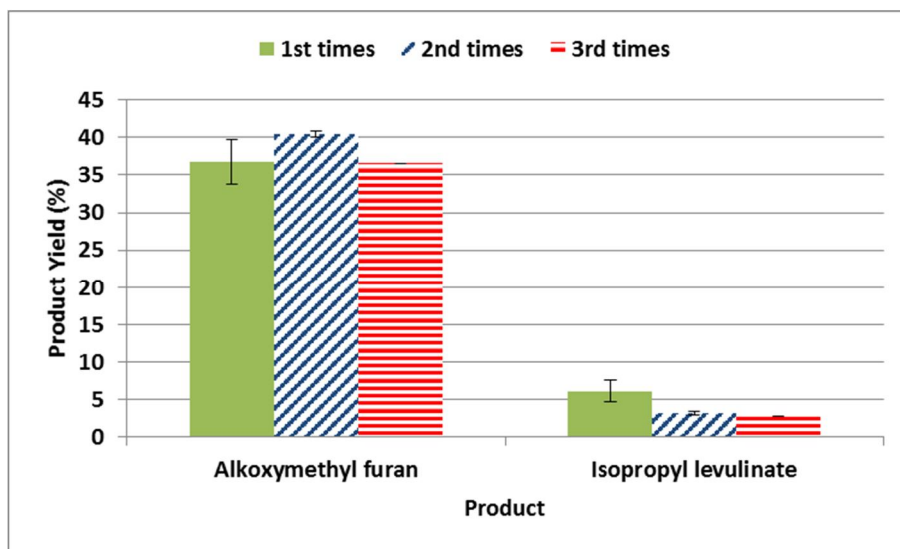


Figure 13. Alkoxyethyl formation by reuse Sn-BEA

5. Conclusion

In this study, the one-pot conversions from glucose to EMF and xylose to alkoxyethyl furan were conducted. To improve Lewis acidity, zeolite was modified by impregnation of tin metal after dealumination process (Sn-BEA) production.

X-ray diffraction analysis for measuring crystalline structure changes of zeolite during zeolite modification process was conducted and revealed that crystalline structure after the modification. X-ray fluorescence analysis was conducted to measure Si/Al ratio change after dealumination process. As a result Si/Al ratio increased from 38 to 520. BET surface area and pore volume analysis of zeolite was conducted, resulting in increasing of surface area due to increase of micropores, while pore volume was relatively constant due to preservation of mesopores structure. And acidic properties of zeolites was measured by NH_3 -TPD analysis, indicating that Brønsted acidity was decreased as modification proceeded due to loss of hydrogen bond formed from SiOAl in zeolite.

To improve yield of EMF from glucose, Lewis acid was required to isomerize glucose to fructose and Brønsted acid was required to dehydration of fructose to 5-HMF and subsequent etherification of 5-HMF to EMF. In case of xylose, Brønsted acid was required to dehydration of xylose to furfural, and Lewis acid was also required for reduction of furfural to furfuryl alcohol and subsequent etherification of furfuryl alcohol to alkoxyethyl furan.

Based on those reaction mechanisms, Sn-BEA (Lewis acid) and Amberlyst 15 (Brønsted acid) were into reaction at the same time and highest yield of EMF was accomplished at reaction temperature 190°C for 10 min.

Alkoxyethyl furan conversion from furfural conducted at reaction temperature from 170 to 190°C , 10 min of reaction time, and Sn-BEA (0.05 g)

as a catalyst. Highest alkoxyethyl furan yield (36.73%) achieved at 190°C of reaction temperature by MPV reduction of furfural to furfuryl alcohol followed by etherification of furfuryl alcohol. On the other hand, xylose to alkoxyethyl furan conversion showed poor results, no alkoxyethyl furan was detected. There were some factors that inhibit subsequent reaction from xylose to alkoxyethyl furan: 1) Strong Lewis acidity converted xylose to lactate instead of furfural to furfuryl alcohol reduction, 2) Propylene formation derived from Brønsted acid catalyzed dehydration of 2-propanol, resulting in preventing furfural reduction by etherification with 2-propanol. Zeolite reusability tests were performed by estimating alkoxyethyl furan yield from furfural. As a result, performance of Sn-BEA remained until two time uses, and slightly decreased in three time uses.

6. References

- Agarwal, A.K. 2007. Biofuels (alcohols and biodiesel) applications as fuels for internal combustion engines. *Progress in Energy and Combustion Science*, **33**(3), 233-271.
- Ahmad, E., Alam, M.I., Pant, K.K., Haider, M.A. 2016. Catalytic and mechanistic insights into the production of ethyl levulinate from biorenewable feedstocks. *Green Chemistry*, **18**(18), 4804-4823.
- Akbar, S. 2010. Characterization of Beta Zeolites by X-Ray Diffraction, Scanning Electron Microscope, and Refractive Index Techniques. *Journal of the Chemical Society of Pakistan*, **32**(5), 592-598.
- Alipour, S., Omidvarborna, H., Kim, D.S. 2017. A review on synthesis of alkoxyethyl furfural, a biofuel candidate. *Renewable & Sustainable Energy Reviews*, **71**, 908-926.
- Alonso, D.M., Bond, J.Q., Serrano-Ruiz, J.C., Dumesic, J.A. 2010. Production of liquid hydrocarbon transportation fuels by oligomerization of biomass-derived C-9 alkenes. *Green Chemistry*, **12**(6), 992-999.
- Antunes, M.M., Lima, S., Neves, P., Magalhaes, A.L., Fazio, E., Fernandes, A., Neri, F., Silva, C.M., Rocha, S.M., Eiro, M.F.R., Pillinger, M., Urakawa, A., Valente, A.A. 2015. One-pot conversion of furfural to useful bio-products in the presence of a Sn,Al-containing zeolite beta catalyst prepared via post-synthesis routes. *Journal of Catalysis*, **329**, 522-537.
- Balakrishnan, M., Sacia, E.R., Bell, A.T. 2012. Etherification and reductive etherification of 5-(hydroxymethyl)furfural: 5-(alkoxyethyl)furfurals and 2,5-bis(alkoxyethyl)furans as potential bio-diesel candidates. *Green Chemistry*, **14**(6), 1626-1634.
- Baran, R., Onfroy, T., Casale, S., Dzwigaj, S. 2014. Introduction of Co into the Vacant T-Atom Sites of SiBEA Zeolite as Isolated Mononuclear Co Species. *Journal of Physical Chemistry C*, **118**(35), 20445-20451.
- Barbera, K., Lanzafame, P., Pistone, A., Millesi, S., Malandrino, G., Gulino, A., Perathoner, S., Centi, G. 2015. The role of oxide location in HMF etherification with ethanol over sulfated ZrO₂ supported on SBA-15. *Journal of Catalysis*, **323**, 19-32.
- Bui, L., Luo, H., Gunther, W.R., Roman-Leshkov, Y. 2013. Domino Reaction Catalyzed by Zeolites with Brønsted and Lewis Acid Sites for the Production of γ -Valerolactone from Furfural. *Angewandte Chemie-International Edition*, **52**(31), 8022-8025.
- Carrasquillo-Flores, R., Kaldstrom, M., Schuth, F., Dumesic, J.A., Rinaldi, R. 2013. Mechanocatalytic Depolymerization of Dry (Ligno)cellulose As an Entry Process for High-Yield Production of Furfurals. *ACS*

- Catalysis*, **3**(5), 993-997.
- Chia, M., Dumesic, J.A. 2011. Liquid-phase catalytic transfer hydrogenation and cyclization of levulinic acid and its esters to gamma-valerolactone over metal oxide catalysts. *Chemical Communications*, **47**(44), 12233-12235.
- Cho, A., Kim, H., Iino, A., Takagaki, A., Oyama, S.T. 2014. Kinetic and FTIR studies of 2-methyltetrahydrofuran hydrodeoxygenation on Ni₂P/SiO₂. *Journal of Catalysis*, **318**, 151-161.
- Choudhary, V., Mushrif, S.H., Ho, C., Anderko, A., Nikolakis, V., Marinkovic, N.S., Frenkel, A.I., Sandler, S.I., Vlachos, D.G. 2013. Insights into the Interplay of Lewis and Bronsted Acid Catalysts in Glucose and Fructose Conversion to 5-(Hydroxymethyl)furfural and Levulinic Acid in Aqueous Media. *Journal of the American Chemical Society*, **135**(10), 3997-4006.
- Corma, A., Iborra, S., Velty, A. 2007. Chemical routes for the transformation of biomass into chemicals. *Chemical Reviews*, **107**(6), 2411-2502.
- Deka, R.C. 1998. Acidity in zeolites and their characterization by different spectroscopic methods. *Indian Journal of Chemical Technology*, **5**(3), 109-123.
- Dijkmans, J., Gabriels, D., Dusselier, M., de Clippel, F., Vanelderen, P., Houthoofd, K., Malfliet, A., Pontikes, Y., Sels, B.F. 2013. Productive sugar isomerization with highly active Sn in dealuminated beta zeolites. *Green Chemistry*, **15**(10), 2777-2785.
- Elliot, S.G., Andersen, C., Tolborg, S., Meier, S., Sadaba, I., Dugaard, A.E., Taarning, E. 2017. Synthesis of a novel polyester building block from pentoses by tin-containing silicates. *Rsc Advances*, **7**(2), 985-996.
- Escobar, J.C., Lora, E.S., Venturini, O.J., Yanez, E.E., Castillo, E.F., Almazan, O. 2009. Biofuels: Environment, technology and food security. *Renewable & Sustainable Energy Reviews*, **13**(6-7), 1275-1287.
- Gandarias, I., Fernandez, S.G., El Doukkali, M., Reques, J., Arias, P.L. 2013. Physicochemical Study of Glycerol Hydrogenolysis Over a Ni-Cu/Al₂O₃ Catalyst Using Formic Acid as the Hydrogen Source. *Topics in Catalysis*, **56**(11), 995-1007.
- Gandarias, I., Reques, J., Arias, P.L., Armbruster, U., Martin, A. 2012. Liquid-phase glycerol hydrogenolysis by formic acid over Ni-Cu/Al₂O₃ catalysts. *Journal of Catalysis*, **290**, 79-89.
- Gilkey, M.J., Panagiotopoulou, P., Mironenko, A.V., Jenness, G.R., Vlachos, D.G., Xu, B.J. 2015. Mechanistic Insights into Metal Lewis Acid-Mediated Catalytic Transfer Hydrogenation of Furfural to 2-Methylfuran. *Acs Catalysis*, **5**(7), 3988-3994.
- Girisuta, B., Janssen, L.P.B.M., Heeres, H.J. 2006. A kinetic study on the decomposition of 5-hydroxymethylfurfural into levulinic acid. *Green Chemistry*, **8**(8), 701-709.

- Gutmann, V. 1978. *The donor-acceptor approach to molecular interactions*. Plenum Press, New York.
- Heinichen, H.K., Holderich, W.F. 1999. Acylation of 2-methoxynaphthalene in the presence of modified zeolite HBEA. *Journal of Catalysis*, **185**(2), 408-414.
- Hernandez, B., Iglesias, J., Morales, G., Paniagua, M., Lopez-Aguado, C., Fierro, J.L.G., Wolf, P., Hermans, I., Melero, J.A. 2016. One-pot cascade transformation of xylose into gamma-valerolactone (GVL) over bifunctional Bronsted-Lewis Zr-Al -beta zeolite. *Green Chemistry*, **18**(21), 5777-5781.
- Hodala, J.L., Halgeri, A.B., Shanbhag, G.V. 2016. Enhancement in activity and shape selectivity of zeolite BEA by phosphate treatment for 2-methoxynaphthalene acylation. *Rsc Advances*, **6**(93), 90579-90586.
- Holm, M.S., Saravanamurugan, S., Taarning, E. 2010. Conversion of Sugars to Lactic Acid Derivatives Using Heterogeneous Zeotype Catalysts. *Science*, **328**(5978), 602-605.
- Horvath, B., Hronec, M., Vavra, I., Sustek, M., Krizanova, Z., Derer, J., Dobrocka, E. 2013. Direct gas-phase epoxidation of propylene over nanostructured molybdenum oxide film catalysts. *Catalysis Communications*, **34**, 16-21.
- Hronec, M., Fulajtarova, K., Liptaj, T. 2012. Effect of catalyst and solvent on the furan ring rearrangement to cyclopentanone. *Applied Catalysis a-General*, **437**, 104-111.
- Hu, X., Lievens, C., Larcher, A., Li, C.Z. 2011. Reaction pathways of glucose during esterification: Effects of reaction parameters on the formation of humin type polymers. *Bioresource Technology*, **102**(21), 10104-10113.
- Jae, J., Mahmoud, E., Lobo, R.F., Vlachos, D.G. 2014. Cascade of Liquid-Phase Catalytic Transfer Hydrogenation and Etherification of 5-Hydroxymethylfurfural to Potential Biodiesel Components over Lewis Acid Zeolites. *Chemcatchem*, **6**(2), 508-513.
- Jae, J., Zheng, W.Q., Lobo, R.F., Vlachos, D.G. 2013. Production of Dimethylfuran from Hydroxymethylfurfural through Catalytic Transfer Hydrogenation with Ruthenium Supported on Carbon. *Chemsuschem*, **6**(7), 1158-1162.
- Jeong, H., Jang, S.K., Hong, C.Y., Kim, S.H., Lee, S.Y., Lee, S.M., Choi, J.W., Choi, I.G. 2017. Levulinic acid production by two-step acid-catalyzed treatment of *Quercus mongolica* using dilute sulfuric acid. *Bioresource Technology*, **225**, 183-190.
- Johnston, C.M.T., van Kooten, G.C. 2015. Back to the past: Burning wood to save the globe. *Ecological Economics*, **120**, 185-193.
- Kamm, B., Kamm, M. 2004. Principles of biorefineries. *Applied Microbiology and Biotechnology*, **64**(2), 137-145.

- Koehle, M., Lobo, R.F. 2016. Lewis acidic zeolite Beta catalyst for the Meerwein-Ponndorf-Verley reduction of furfural. *Catalysis Science & Technology*, **6**(9), 3018-3026.
- Kondo, J.N., Nishitani, R., Yoda, E., Yokoi, T., Tatsumi, T., Domen, K. 2010. A comparative IR characterization of acidic sites on HY zeolite by pyridine and CO probes with silica-alumina and gamma-alumina references. *Physical Chemistry Chemical Physics*, **12**(37), 11576-11586.
- Kumar, P., Barrett, D.M., Delwiche, M.J., Stroeve, P. 2009. Methods for Pretreatment of Lignocellulosic Biomass for Efficient Hydrolysis and Biofuel Production. *Industrial & Engineering Chemistry Research*, **48**(8), 3713-3729.
- Lanzafame, P., Barbera, K., Perathoner, S., Centi, G., Aloise, A., Migliori, M., Macario, A., Nagy, J.B., Giordano, G. 2015. The role of acid sites induced by defects in the etherification of HMF on Silicalite-1 catalysts. *Journal of Catalysis*, **330**, 558-568.
- Lanzafame, P., Temi, D.M., Perathoner, S., Centi, G., Macario, A., Aloise, A., Giordano, G. 2011. Etherification of 5-hydroxymethyl-2-furfural (HMF) with ethanol to biodiesel components using mesoporous solid acidic catalysts. *Catalysis Today*, **175**(1), 435-441.
- Lew, C.M., Rajabbeigi, N., Tsapatsis, M. 2012. One-Pot Synthesis of 5-(Ethoxymethyl)furfural from Glucose Using Sn-BEA and Amberlyst Catalysts. *Industrial & Engineering Chemistry Research*, **51**(14), 5364-5366.
- Lewis, J.D., Van de Vyver, S., Crisci, A.J., Gunther, W.R., Michaelis, V.K., Griffin, R.G., Roman-Leshkov, Y. 2014. A Continuous Flow Strategy for the Coupled Transfer Hydrogenation and Etherification of 5-(Hydroxymethyl)furfural using Lewis Acid Zeolites. *Chemsuschem*, **7**(8), 2255-2265.
- Li, H., Saravanamurugan, S., Yang, S., Riisager, A. 2016. Direct transformation of carbohydrates to the biofuel 5-ethoxymethylfurfural by solid acid catalysts. *Green Chemistry*, **18**(3), 726-734.
- Li, H.C., Wang, J., Zhou, D.H., Tian, D.X., Shi, C., Mueller, U., Feyen, M., Gies, H., Xiao, F.S., De Vos, D., Yokoi, T., Bao, X.H., Zhang, W.P. 2015. Structural stability and Lewis acidity of tetravalent Ti, Sn, or Zr-linked interlayer-expanded zeolite COE-4: A DFT study. *Microporous and Mesoporous Materials*, **218**, 160-166.
- Li, H.X., Luo, H.S., Zhuang, L., Dai, W.L., Qiao, M.H. 2003. Liquid phase hydrogenation of furfural to furfuryl alcohol over the Fe-promoted Ni-B amorphous alloy catalysts. *Journal of Molecular Catalysis a-Chemical*, **203**(1-2), 267-275.
- Liaw, B.J., Chiang, S.J., Chen, S.W., Chen, Y.Z. 2008. Preparation and catalysis of amorphous CoNiB and polymer-stabilized CoNiB

- catalysts for hydrogenation of unsaturated aldehydes. *Applied Catalysis a-General*, **346**(1-2), 179-188.
- Liu, B., Zhang, Z.H., Huang, K.C. 2013a. Cellulose sulfuric acid as a bio-supported and recyclable solid acid catalyst for the synthesis of 5-hydroxymethylfurfural and 5-ethoxymethylfurfural from fructose. *Cellulose*, **20**(4), 2081-2089.
- Liu, B., Zhang, Z.H., Huang, K.C., Fang, Z.F. 2013b. Efficient conversion of carbohydrates into 5-ethoxymethylfurfural in ethanol catalyzed by AlCl₃. *Fuel*, **113**, 625-631.
- Maache, M., Janin, A., Lavalley, J.C., Joly, J.F., Benazzi, E. 1993. Acidity of Zeolites-Beta Dealuminated by Acid Leaching - an Ftir Study Using Different Probe Molecules (Pyridine, Carbon-Monoxide). *Zeolites*, **13**(6), 419-426.
- Marakatti, V.S., Halgeri, A.B. 2015. Metal ion-exchanged zeolites as highly active solid acid catalysts for the green synthesis of glycerol carbonate from glycerol. *Rsc Advances*, **5**(19), 14286-14293.
- Mariscal, R., Maireles-Torres, P., Ojeda, M., Sadaba, I., Granados, M.L. 2016. Furfural: a renewable and versatile platform molecule for the synthesis of chemicals and fuels. *Energy & Environmental Science*, **9**(4), 1144-1189.
- Moreno-Recio, M., Santamaria-Gonzalez, J., Maireles-Torres, P. 2016. Bronsted and Lewis acid ZSM-5 zeolites for the catalytic dehydration of glucose into 5-hydroxymethylfurfural. *Chemical Engineering Journal*, **303**, 22-30.
- Neves, P., Antunes, M.M., Russo, P.A., Abrantes, J.P., Lima, S., Fernandes, A., Pillinger, M., Rocha, S.M., Ribeiro, M.F., Valente, A.A. 2013. Production of biomass-derived furanic ethers and levulinate esters using heterogeneous acid catalysts. *Green Chemistry*, **15**(12), 3367-3376.
- Niwa, M., Katada, N., Okumura, K. 2010. *Characterization and design of zeolite catalysts : solid acidity, shape selectivity and loading properties*. Springer-Verlag, Heidelberg ; New York.
- Nyalosaso, J.L., Derrien, G., Charnay, C., de Menorval, L.C., Zajac, J. 2012. Aluminium-derivatized silica monodisperse nanospheres by a one-step synthesis-functionalization method and application as acid catalysts in liquid phase. *Journal of Materials Chemistry*, **22**(4), 1459-1468.
- Octave, S., Thomas, D. 2009. Biorefinery: Toward an industrial metabolism. *Biochimie*, **91**(6), 659-664.
- Ogbonna, J.C., Mashima, H., Tanaka, H. 2001. Scale up of fuel ethanol production from sugar beet juice using loofa sponge immobilized bioreactor. *Bioresource Technology*, **76**(1), 1-8.
- Ordonsky, V.V., Schouten, J.C., van der Schaaf, J., Nijhuis, T.A. 2013.

- Biphasic single-reactor process for dehydration of xylose and hydrogenation of produced furfural. *Applied Catalysis a-General*, **451**, 6-13.
- Pagan-Torres, Y.J., Wang, T.F., Gallo, J.M.R., Shanks, B.H., Dumesic, J.A. 2012. Production of 5-Hydroxymethylfurfural from Glucose Using a Combination of Lewis and Bronsted Acid Catalysts in Water in a Biphasic Reactor with an Alkylphenol Solvent. *Acs Catalysis*, **2**(6), 930-934.
- Panagiotopoulou, P., Martin, N., Vlachos, D.G. 2014. Effect of hydrogen donor on liquid phase catalytic transfer hydrogenation of furfural over a Ru/RuO₂/C catalyst. *Journal of Molecular Catalysis a-Chemical*, **392**, 223-228.
- Panagiotopoulou, P., Vlachos, D.G. 2014. Liquid phase catalytic transfer hydrogenation of furfural over a Ru/C catalyst. *Applied Catalysis a-General*, **480**, 17-24.
- Roberge, D.M., Hausmann, H., Holderich, W.F. 2002. Dealumination of zeolite beta by acid leaching: a new insight with two-dimensional multi-quantum and cross polarization Al-27 MAS NMR. *Physical Chemistry Chemical Physics*, **4**(13), 3128-3135.
- Roman-Leshkov, Y., Barrett, C.J., Liu, Z.Y., Dumesic, J.A. 2007. Production of dimethylfuran for liquid fuels from biomass-derived carbohydrates. *Nature*, **447**(7147), 982-U5.
- Roy, S., Bakhmutsky, K., Mahmoud, E., Lobo, R.F., Gorte, R.J. 2013. Probing Lewis Acid Sites in Sn-Beta Zeolite. *Acs Catalysis*, **3**(4), 573-580.
- Sacia, E.R., Balakrishnan, M., Bell, A.T. 2014. Biomass conversion to diesel via the etherification of furanyl alcohols catalyzed by Amberlyst-15. *Journal of Catalysis*, **313**, 70-79.
- Saravanamurugan, S., Paniagua, M., Melero, J.A., Riisager, A. 2013. Efficient Isomerization of Glucose to Fructose over Zeolites in Consecutive Reactions in Alcohol and Aqueous Media. *Journal of the American Chemical Society*, **135**(14), 5246-5249.
- Seo, G., Chon, H. 1981. Hydrogenation of Furfural over Copper-Containing Catalysts. *Journal of Catalysis*, **67**(2), 424-429.
- Singh, A., Pant, D., Korres, N.E., Nizami, A.S., Prasad, S., Murphy, J.D. 2010. Key issues in life cycle assessment of ethanol production from lignocellulosic biomass: Challenges and perspectives. *Bioresource Technology*, **101**(13), 5003-5012.
- Srivastava, R., Iwasa, N., Fujita, S., Arai, M. 2009. Dealumination of Zeolite Beta Catalyst Under Controlled Conditions for Enhancing its Activity in Acylation and Esterification. *Catalysis Letters*, **130**(3-4), 655-663.
- Stevens, J.G., Bourne, R.A., Twigg, M.V., Poliakoff, M. 2010. Real-Time Product Switching Using a Twin Catalyst System for the Hydrogenation of Furfural in Supercritical CO₂. *Angewandte*

Chemie-International Edition, **49**(47), 8856-8859.

- Taarning, E., Osmundsen, C.M., Yang, X.B., Voss, B., Andersen, S.I., Christensen, C.H. 2011. Zeolite-catalyzed biomass conversion to fuels and chemicals. *Energy & Environmental Science*, **4**(3), 793-804.
- Triantafyllidis, K.S., Evmiridis, N.P. 2000. Dealuminated H-Y zeolites: Influence of the number and type of acid sites on the catalytic activity for isopropanol dehydration. *Industrial & Engineering Chemistry Research*, **39**(9), 3233-3240.
- Vargas-Hernandez, D., Rubio-Caballero, J.M., Santamaria-Gonzalez, J., Moreno-Tost, R., Merida-Robles, J.M., Perez-Cruz, M.A., Jimenez-Lopez, A., Hernandez-Huesca, R., Maireles-Torres, P. 2014. Furfuryl alcohol from furfural hydrogenation over copper supported on SBA-15 silica catalysts. *Journal of Molecular Catalysis a-Chemical*, **383**, 106-113.
- Viswanadham, N., Kumar, M. 2006. Effect of dealumination severity on the pore size distribution of mordenite. *Microporous and Mesoporous Materials*, **92**(1-3), 31-37.
- Xu, W.J., Xia, Q.N., Zhang, Y., Guo, Y., Wang, Y.Q., Lu, G.Z. 2011. Effective Production of Octane from Biomass Derivatives under Mild Conditions. *Chemsuschem*, **4**(12), 1758-1761.
- Yang, W.R., Sen, A. 2011. Direct Catalytic Synthesis of 5-Methylfurfural from Biomass-Derived Carbohydrates. *Chemsuschem*, **4**(3), 349-352.
- Yang, Y., Abu-Omar, M.M., Hu, C.W. 2012. Heteropolyacid catalyzed conversion of fructose, sucrose, and inulin to 5-ethoxymethylfurfural, a liquid biofuel candidate. *Applied Energy*, **99**, 80-84.
- Yi, G.S., Zhang, Y.G. 2012. One-Pot Selective Conversion of Hemicellulose (Xylan) to Xylitol under Mild Conditions. *Chemsuschem*, **5**(8), 1383-1387.
- Yu, Z.W., Li, S.H., Wang, Q., Zheng, A.M., Jun, X., Chen, L., Deng, F. 2011. Bronsted/Lewis Acid Synergy in H-ZSM-5 and H-MOR Zeolites Studied by H-1 and Al-27 DQ-MAS Solid-State NMR Spectroscopy. *Journal of Physical Chemistry C*, **115**(45), 22320-22327.
- Zhang, K., Pei, Z.J., Wang, D.H. 2016. Organic solvent pretreatment of lignocellulosic biomass for biofuels and biochemicals: A review. *Bioresource Technology*, **199**, 21-33.
- Zhang, Z.H., Deng, K.J. 2015. Recent Advances in the Catalytic Synthesis of 2,5-Furandicarboxylic Acid and Its Derivatives. *Acs Catalysis*, **5**(11), 6529-6544.

초 록

고형 산촉매 개질을 통한 글루코오스 및 자일로오스 유래 퓨란계 화합물 전환 연구

김종화

환경재료과학전공

산림과학부

서울대학교 대학원

퓨란계 화합물은 차세대 바이오연료 및 화학물질로써 그 활용 가치가 높아 주목 받고 있다. 특히 Ethoxymethyl furfural (EMF)과 alkoxymethyl furan은 바이오에탄올과 비교했을 때 (6.1 kWh/l, 20 MJ/kg) 높은 연료 물성을 띄어 주목 받고 있다 (EMF: 8.7 kWh/l, alkoxymethyl furan: 27 MJ/kg).

본 연구에서는 글루코오스와 자일로오스의 one-pot 전환 반응을 통해 각각 EMF, alkoxymethyl furan을 생산하였다. 촉매로는 Brønsted acid인 Amberlyst 15와 주석 첨가를 통해 Lewis acid를 띤 제올라이트 베타를 사용하였다. 제올라이트 베타는 알루미늄 제거 반응과 주석 첨가 반응을 통해 개질 되어 Sn-BEA로 명명하였다. 개질된 제올라이트의 mesopores는 그대로 유지되었으며 알루미늄 제거로 인해 Si/Al 비율은 38에서 520까지 증가하였다. X-ray diffraction 결과 제올라이트 개질 이후에도 제올라이트의

결정 구조는 크게 바뀌지 않은 것을 확인하였다. 제올라이트와 Amberlyst 15의 산 촉매 특성은 NH_3 -Temperature programmed desorption을 통해 측정되었으며 제올라이트 개질에 따라 Brønsted 특성이 감소하는 것으로 확인되었다.

글루코오스로부터 EMF로의 One-pot 전환 반응의 반응조건은 반응온도 180-200°C, 반응시간 10-30분 촉매는 Sn-BEA (0.025 g)+Amberlyst 15 (0.025 g), Amberlyst 15 (0.05 g), Sn-BEA (0.05 g)을 사용하였다. EMF의 최대 생산 수율은 반응온도 190°C, 반응시간 10분, Sn-BEA+Amberlyst 15 조건에서 29.37%를 달성하였다. 상기 조건에서 촉매 비율을 달리하여 실험한 결과 Sn-BEA와 Amberlyst 15의 질량비가 1:1일 때 EMF의 수율이 가장 높은 것으로 확인되었다. 자일로오스로부터 alkoxyethyl furan으로의 one-pot 전환 반응의 조건은 반응온도 170-190°C, 반응시간은 10분으로 설정되었고 촉매는 앞선 글루코오스의 전환 조건과 동일하게 설정되었다. 실험 결과 propylene, lactate와 같은 경쟁 산물의 발생으로 alkoxyethyl furan의 생산이 확인되지 않았다. 촉매의 재사용 실험은 furfural로부터 alkoxyethyl furan의 전환 반응을 통해 평가되었고 두 번째 사용까지는 활성이 유지되었으나 세 번째부터 활성이 약간 감소하였음이 확인되었다.

주요어: 글루코오스, 자일로오스, one-pot반응, EMF, alkoxyethyl furan, 베타 제올라이트, Amberlyst 15, 제올라이트 개질

학번: 2015-23019